Chem. Soc. Rev., 1990, **19**, 439–470

Dynamic Decay Properties of Excited Electronic States of Polyatomic Molecular Ions Studied with Synchrotron Radiation

By Richard P. Tuckett
SCHOOL OF CHEMISTRY, THE UNIVERSITY OF BIRMINGHAM, EDGBASTON, BIRMINGHAM B15 2TT

1 Introduction

This review is concerned with a family of polyatomic molecular ions whose excited valence electronic states show interesting and unexpected decay properties. The species of interest are the halogenated ions of group IV of the periodic table, and we are now extending these studies to group III cations. They have valence states which lie 10—30 eV above the ground state of the neutral molecule, and this article will describe experiments using tunable vacuum ultra-violet (VUV) radiation from a synchrotron as a photoionization source to measure the different decay properties of these states.

Molecular ions are transient, free radicals whose importance in comets, interstellar space, and flame chemistry (to name but three examples) is now widely appreciated, and the past 15 years has seen an enormous growth in techniques to study both their spectroscopic and dynamic properties. The different spectroscopic techniques which can now cover a huge range of the electromagnetic spectrum was the subject of a Royal Society Discussion meeting in 1987[1] and advancements in electronic spectroscopy were described by Maier in a recent edition of the *Chemical Society Reviews*.[2] In any spectroscopic experiment the primary aim is to produce as high a concentration of the molecular ion (in this case) of interest as possible, and the presence of unwanted species is not important so long as they do not mask the spectral features (*i.e.* line positions and intensities) of the ion. This goes a long way to explaining why electron impact[3] and many different forms of electrical discharge[4] have been popular methods for producing ions for spectral characterization. Electron impact ionization is an example of what I will refer to as a 'non-resonant' technique, in that the energy of the ionizing electron is often very much greater than that needed to populate the ground state of the ion (for absorption experiments) or an excited state of the ion (for emission or fragmentation experiments). The subsequent fragmentation that can occur in a polyatomic ion (to both neutral and ionic fragments) is compensated by the large cross-sections for electron impact ionization. Therefore, so long as spectral masking does not occur, this

[1] Royal Society Discussion Meeting on the Spectroscopy of Molecular Ions, *Philos. Trans. R. Soc. London, A* 1988, vol. 324.
[2] J. P. Maier, *Chem. Soc. Rev.*, 1988, **17**, 45.
[3] J. P. Maier, *Chimia*, 1980, **34**, 219.
[4] G. Herzberg, *Quart. Rev. Chem. Soc.*, 1971, **25**, 201.

method is excellent at producing a high concentration of ions for spectral characterization. The absolute value of the concentration is not important.

A dynamics experiment has different requirements. To study the decay of an isolated state of a gas phase species, the aim now is to produce only that state of the ion to be studied and ideally with a known concentration or flux. A non-resonant excitation source such as electrons can no longer be used and techniques using photons are usually employed. In the study of singly-charged molecular ions with electronic states of energy less than 21.2 eV above the ground state of the parent neutral molecule, photoionization using the He-I line at 584 Å (or 21.2 eV) from a helium discharge lamp is often used:

$$AB_n \xrightarrow{\text{He-I}} (AB_n)^{+(*)} + e^- \qquad (1)$$

AB_n is a generalized, polyatomic molecule and the asterisk represents an excited electronic state. Photoionization of this kind is a non-resonant process because the electron can carry away the energy difference between the He-I photon and the energy of $(AB_n)^{+(*)}$ as excess kinetic energy. The concentration of ion produced is then determined by the partial ionization cross-section of that electronic state for an incident photon energy of 21.2 eV. An electron energy analyser is often used to define the kinetic energy (KE) of the ejected electron and by this way the state of the ion $(AB_n)^+$ to be studied is defined uniquely. A range of coincidence techniques have been developed to measure dynamic decay properties of such isolated states of molecular ions. These include the photoion–fluorescence photon (PIFCO) technique,[5] the photoelectron–photoion (PEPICO) technique,[6] and the photoelectron–fluorescence photon (PEFCO) technique.[7] The decay properties measured have included fluorescence quantum yields, radiative lifetimes, and non-radiative unimolecular decay rates of isolated electronic states of polyatomic ions. Such measurements are now being extended to doubly-charged molecular ions produced by non-resonant photoionization using the He-II line at 40.8 eV.[8]

Such techniques suffer two disadvantages. Firstly, in the case of He-I photoionization, the ionic states that can be studied are limited to those with energy less than 21.2 eV. Secondly, the resolution of the experiment (*i.e.* the spectral width of the ionic state whose decay properties we wish to investigate) is limited by that of the electron energy analyser, and this often means that only widely spaced vibrational features within an electronic state manifold can be distinguished. In theory both problems can be circumvented using tunable VUV radiation from a synchrotron as a 'resonant' photoionization source:

$$AB_n \xrightarrow{h\nu} (AB_n)^{+(*)} + e^- \qquad (2)$$

[5] S Leach, *J Mol Struct*, 1984, **141**, 43
[6] T Baer, *Adv Chem Phys*, 1986, **64**, 111
[7] J P Maier and F Thommen, in 'Gas-Phase Ion Chemistry', Vol 3, 'Ions and Light', ed M T Bowers, Academic Press, London, 1984, p 357
[8] D M Curtis and J H D Eland, *Int J Mass Spectrom Ion Phys*, 1985, **63**, 241

This review describes such experiments. Neutral, polyatomic molecules are photoionized by radiation from the Science and Engineering Research Council Daresbury synchrotron source, and the competing radiative and non-radiative decay channels of excited electronic states of $(AB_n)^+$ are investigated by two complementary techniques:

$$(AB_n)^{+(*)} \xrightarrow{k_{rad}} (AB_n)^+ + h\nu$$

$$\text{or } (AB_n)^{+(*)} \xrightarrow{k_{non\text{-}rad}} \text{fragment ions} \qquad (3)$$

The competition between these pathways lies at the heart of our understanding of molecular dynamics, and this review describes these processes for a range of polyatomic systems, namely the cations of the pure and mixed halides of group IV of the periodic table.

The radiative decay of $(AB_n)^{+(*)}$ (occurring at a rate k_{rad}) is measured in a relatively simple crossed gas spray–tunable VUV beam apparatus with undispersed fluorescence detection.[9] Non-radiative fragmentation of $(AB_n)^{+(*)}$ (occurring at a rate $k_{non\text{-}rad}$) is measured in a more complicated energy scanning PEPICO apparatus,[10] which is in effect a novel form of photoionization mass spectrometry. In the radiative decay experiment, thresholds for fluorescence are determined, and in favourable cases an estimate of the fluorescence quantum yield $\Phi_{h\nu}$ or (more accurately) radiative probability of the excited electronic state can be made. Using the synchrotron in its pulsed mode (see Section 2) radiative lifetimes τ can be measured very accurately. Since $\Phi_{h\nu} = k_{rad}/(k_{rad} + k_{non\text{-}rad})$ and $\tau^{-1} = (k_{rad} + k_{non\text{-}rad})$ changes in $\Phi_{h\nu}$ and τ with excitation energy are especially interesting, since they can usually be attributed to a change in $k_{non\text{-}rad}$, *i.e.* the onset of a competing, non-radiative channel. However the fragment ions produced by such a process are not probed directly. These measurements are made in the energy scanning PEPICO apparatus, again using tunable VUV radiation from a synchrotron source as the means of producing the polyatomic ions.

The Daresbury synchrotron radiation source and the experimental details are described in Section 2. Section 3 reviews earlier 'spectroscopically-based' experiments made in Birmingham on the cations of the halides of group IV, *i.e.* the family of ions built upon CF_4^+. These experiments preceded those at Daresbury, and indicated the value of using a tunable vacuum UV photon source to create ions for dynamics experiments. Section 4 describes the results from the radiative decay experiment, Section 5 from the non-radiative decay experiment, and some general conclusions are made in Section 6.

[9] I. R. Lambert, S. M. Mason, R. P. Tuckett, and A. Hopkirk, *J. Chem. Phys.*, 1988, **89**, 2683.
[10] J. C. Creasey, I. R. Lambert, R. P. Tuckett, K. Codling, L. J. Frasinski, P. A. Hatherly, M. Stankiewicz, and D. M. P. Holland, *J. Chem. Phys.*, 1990, **93**, 3295.

2 Experimental

Several books have been written about the properties of synchrotron sources and the reader is referred to such texts for an understanding of the fundamental physics of these sources. A review of the characteristics of the United Kingdom Synchrotron Radiation Source (SRS) at Daresbury in Cheshire was given by Holland in 1986,[11] and although the number of beam lines and extent of the experiments has increased substantially in the last four years this review still remains an excellent reference to the properties of this source. Briefly, the Daresbury SRS is a 2 GeV electron storage ring which is injected from a 600 MeV synchrotron booster. The ring has a radius of *ca.* 15 m, the electron flight time is *ca.* 320 ns and the ring can accommodate 160 electron bunches in what is generally referred to as the 'multi-bunch' mode. The electron pulse width is *ca.* 200 ps. Tangential to the ring to collect the associated electromagnetic radiation are 13 ports, one of which is dedicated to vacuum UV/soft *X*-ray gas phase molecular physics. Three monochromators serve this port, a normal incidence 1 m Seya, a normal incidence 5 m MacPherson, and a 3 m toroidal grating grazing incidence instrument. The first two operate in the energy range 5—35 eV, the third 20—150 eV. All the experiments described in this review used the Seya monochromator which has a quoted photon flux of 1×10^{11} s^{-1} $Å^{-1}$ at 600 Å. The properties of the SRS that are exploited are directionality, easy energy tunability, and excellent timing properties when only one electron bunch is in the ring (the 'single-bunch' mode which is in effect a pulsed source of electromagnetic radiation, pulse width 200 ps with a repetition rate of *ca.* 3 MHz). The photon beam also has a high degree of linear polarization. Up to now we have not exploited this properly in our work, but future experiments to measure the degree of polarization of fluorescence from polyatomic molecular ions are planned.

Two different experiments are used to investigate radiative and non-radiative decay of electronic states of polyatomic molecular ions and full details can be found elsewhere.[9,10] Common to both experiments, however, is the orthogonal crossing of a gas spray of the neutral molecule with tunable vacuum UV radiation from the 1 m Seya monochromator at the Daresbury ring. The majority of the experiments use photon wavelengths well below the lithium fluoride cut-off of 106 nm, so a windowless, differentially pumped system has to be employed. Thus the radiation is focused out of the exit slit of the Seya into a 2 mm internal diameter 10—45 cm long glass capillary which ends *ca.* 5—10 mm from the crossing region with the gas spray. (The lengths and distances used depend on which experiment is being performed.) The capillary channels the radiation to the interaction region and ensures poor conductance between monochromator and experiment, so only one stage of differential pumping between the Seya and the experimental chamber is needed to maintain the necessary, low pressure of the monochromator. The absolute synchrotron flux in the experimental chamber is measured either by a Al_2O_3 photocathode (in the

[11] D M P Holland, *Phys Scrip*, 1987, **36**, 22

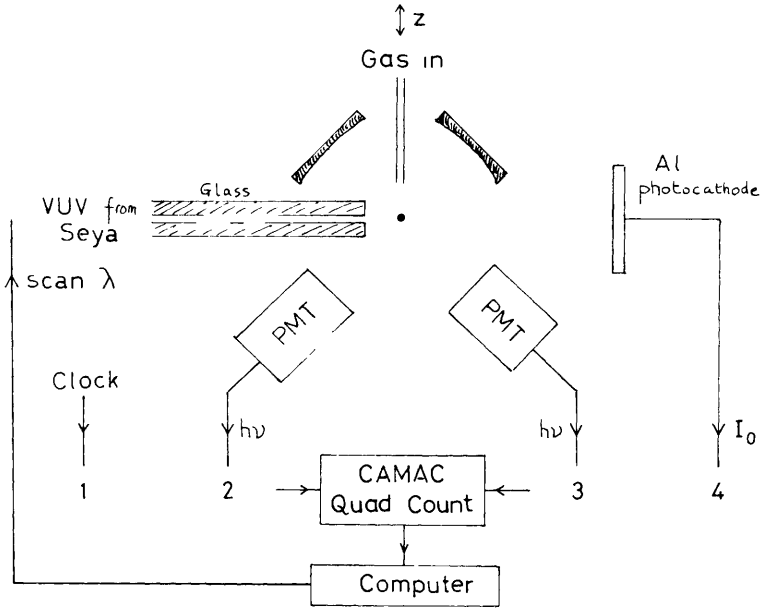

Figure 1 *Diagram of the fluorescence excitation apparatus*

radiative experiment) or by a sodium salicylate coated window plus photomultiplier tube used in the photon counting mode (in the non-radiative experiment). The Seya has two gratings (both with 1200 lines per mm) mounted back-to-back on a single kinematic mount. They are blazed at *ca.* 600 and 900 Å, providing photon flux between 350—850 Å ('high energy' grating) and 700—1200 Å ('low energy' grating) respectively. Second order radiation is only problematic with the high energy grating for $\lambda > 800$ Å, with the low energy grating for $\lambda > 1150$ Å. The ultimate resolution of the Seya is *ca.* 0.5 Å, although the majority of our spectra were recorded at a resolution of 2 Å.

In the radiative decay experiment (Figure 1) undispersed fluorescence from the interaction region is focused by a f/1.3 75 mm focal length concave mirror through a MgF_2 window and a 50 mm square filter onto a photomultiplier tube. Two such tube + filter combinations can be used so that fluorescence in two different spectral regions can simultaneously be detected. The photomultiplier tubes are used in the photon counting mode and the signals are processed by CAMAC electronics and a dedicated LSI 11 mini-computer. Data are transferred to the Daresbury Mainframe Computer (Convex C220) for analysis. Two types of experiment can be performed. In the 'multi-bunch' (or quasi c.w.) mode, the photon wavelength (or energy) is scanned, total fluorescence collected, and fluorescence excitation spectra are recorded. Such experiments measure thresholds for fluorescence, and in favourable cases an estimate of the fluorescence quantum yield of the electronic state can be made. In the 'single-

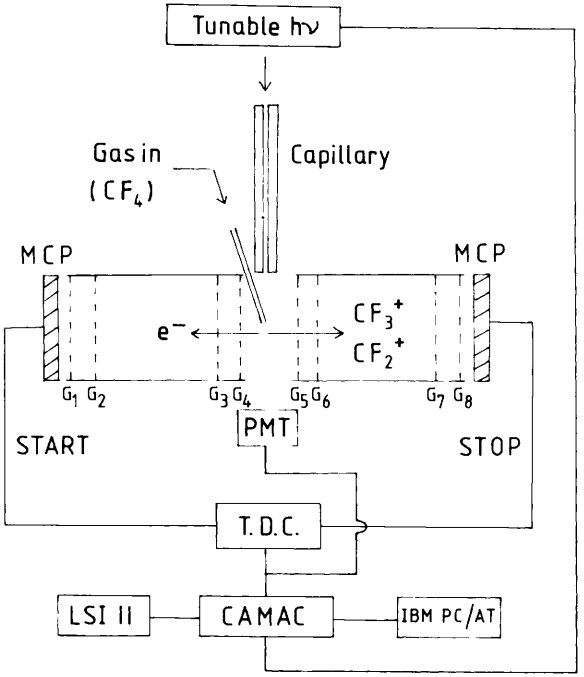

Figure 2 *Diagram of the non-radiative fragmentation apparatus.* G_1—G_8 *are grids on the pair of identical TOF mass spectrometers. MCP = microchannel plates, PMT = photomultiplier tube, TDC = time to digital converter*
(Reproduced by permission from *J. Chem. Phys.*, 1990, **93**, 3296)

bunch' (or pulsed) mode, radiative lifetime measurements are made (see Section 2), and decays can be measured at different photon excitation energies.

In the non-radiative experiment (Figure 2), the interaction region between gas spray and photon beam occurs at the centre of a pair of identical 10 cm long time-of-flight (TOF) mass spectrometers. Electrons are accelerated out of the interaction region to one set of microchannel plates, parent and fragment ions to the other set, the two signals are counted in delayed coincidence by the PEPICO technique, and a TOF mass spectrum is obtained. The photon energy is changed and the experiment repeated. The apparatus is again controlled by CAMAC electronics interfaced to two interacting computers, an IBM PC/AT with colour graphics and an LSI 11/23. The former sets the experimental conditions, displays the data in real time and stores it on disc. Data accumulate as a three-dimensional histogram of photon energy *versus* ion TOF *versus* coincidence count rate, with the last variable represented by colour. The LSI 11 steps the Seya monochromator, stores auxiliary measurements (including the total electron count), and accesses the Daresbury mainframe computer. TOF spectra accumulate normalized to the synchrotron flux (which has to be in the multi-bunch

mode), as described elsewhere.[10] Data can be displayed either as the original 3-D histogram, or by taking cross-sectional cuts through it in one of two ways. Either intensity *versus* ion TOF is displayed at a fixed photon energy, or the intensity of a particular fragment ion is displayed as a function of photon energy (*i.e.* an ion yield curve). If the signal-to-noise ratio is high enough, the latter method is more revealing because it gives directly thresholds for ion fragmentation. The former method is used with weak fragmentation channels (by comparing TOF spectra above and below a certain energy), but the threshold energy is not defined uniquely.

This technique has many similarities to photoionization mass spectrometry (PIMS),[12] but with three main advantages. First, the use of a synchrotron source means that in our experiment wavelengths down to 350 Å can be accessed, whereas most PIMS experiments use a helium continuum and vacuum UV monochromator as the photon source with wavelengths limited to *ca.* $\lambda > 600$ Å. Second, the use of TOF detection means that all the fragment ions are collected simultaneously, and quantitative comparisons can be made between different ions collected in a single experiment. Third, time correlation of the ejected photoelectron with a fragment ion in the TOF mass spectrometer means that the KE release in a fragmentation channel can be measured.[10] The apparatus does however have one principle limitation, in that there is no energy analysis of the photoelectrons; in fact electrons with 0—8 eV kinetic energy are all estimated to be collected with 100% efficiency.[13] Therefore, the electrons which provide the 'start' pulses in the PEPICO experiment can originate from photoionization of AB_n to several different electronic states of $(AB_n)^+$ up to the energy available from the incident VUV photon. Ideally the detected photoelectron would have zero kinetic energy (*i.e.* a threshold electron), then the internal energy state of $(AB_n)^+$ would be uniquely defined (see equation 2). This modification to the apparatus is in progress.

3 Spectroscopic Experiments on Group IV Tetrahalide Molecular Ions

Initial experiments on the spectroscopic properties of excited electronic states of the group IV tetrahalide molecular ions MX_4^+ (M = C,Si,Ge; X = F,Cl,Br) were made at Birmingham in a crossed supersonic beam–electron beam apparatus with dispersed fluorescence detection.[14] The supersonic beam provides substantial rotational, and to a lesser extent vibrational, cooling of the polyatomic parent neutral molecule. The process of non-resonant electron impact ionization involves little transfer of rotational angular momentum, so whereas the vibrational levels within an electronic state of the parent ion of MX_4 are produced with a Franck–Condon distribution, each vibronic state has a very low rotational temperature (typically < 30 K). If this state is bound and decays radiatively by

[12] J. Berkowitz, 'Photoabsorption, Photoionisation, and Photoelectron Spectroscopy', Academic Press, 1979, p. 410; *Radiat. Phys. Chem.*, 1988, **32**, 23.
[13] M. Stankiewicz, P. A. Hatherly, L. J. Frasinski, K. Codling, and D. M. P. Holland, *J. Phys. B*, 1989, **22**, 21.
[14] A. Carrington and R. P. Tuckett, *Chem. Phys. Lett.*, 1980, **74**, 19.

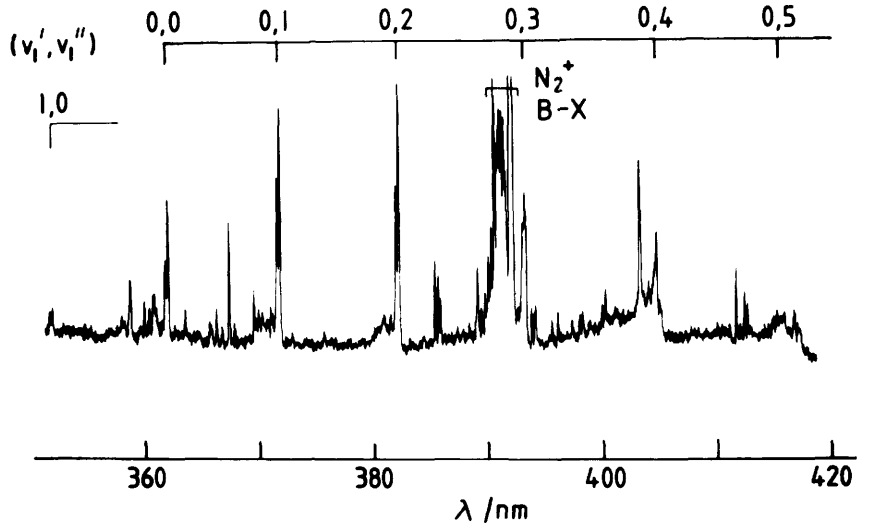

Figure 3 *Spectrum of* CF_4^+ $\tilde{D}\,^2A_1$—$\tilde{C}\,^2T_2$ *resulting from electron impact ionization of* CF_4 *at a low rotational temperature The vibrational assignment* (v_1', v_1'') *is shown*
(Reproduced by permission from *Mol Phys*, 1987, **60**, 763)

photon emission to a lower-lying bound state (a 'bound–bound' transition), the emission spectrum will be condensed into a few rotational components This spectral simplification, compared to the relative complexity of a room temperature source, has been essential for detailed spectroscopic analysis of these polyatomic ions On the other hand, if the lower electronic state to which photon emission occurs is repulsive, fluorescence spectra will only be observed as a broad band 'bound-free' spectrum The spectral width is then a reflection of the repulsive nature of the curve in the Franck–Condon region below the fluorescing bound state, and the rotational simplification afforded by the molecular beam is not utilised We have observed both bound–bound and bound–free spectra in this study of electronic spectra of MX_4^+

A. Bound–Bound Discrete Spectra in MX_4^+.—Bound–bound spectra are observed in the fluorides of MX_4^+, *i e* CF_4^+, SiF_4^+, and Ge_4^+[15–17] and the transition is between the fourth and third excited electronic states of these ions The states have symmetry $\tilde{D}\,^2A_1$ and $\tilde{C}\,^2T_2$ respectively, are connected by an allowed electric dipole tran-sition, and lie *ca* 18—25 eV above the ground state of the parent neutral mol-ecule The main spectroscopic interest has centred on the triply-degenerate $\tilde{C}\,^2T_2$ state This state shows first-order Coriolis splitting, spin–orbit splitting, and has the correct symmetry to distort from tetrahedral geometry

[15] J F M Aarts, S M Mason, and R P Tuckett, *Mol Phys*, 1987, **60**, 761
[16] S M Mason and R P Tuckett, *Mol Phys*, 1987, **60**, 771
[17] S M Mason and R P Tuckett, *Mol Phys*, 1987, **62**, 979

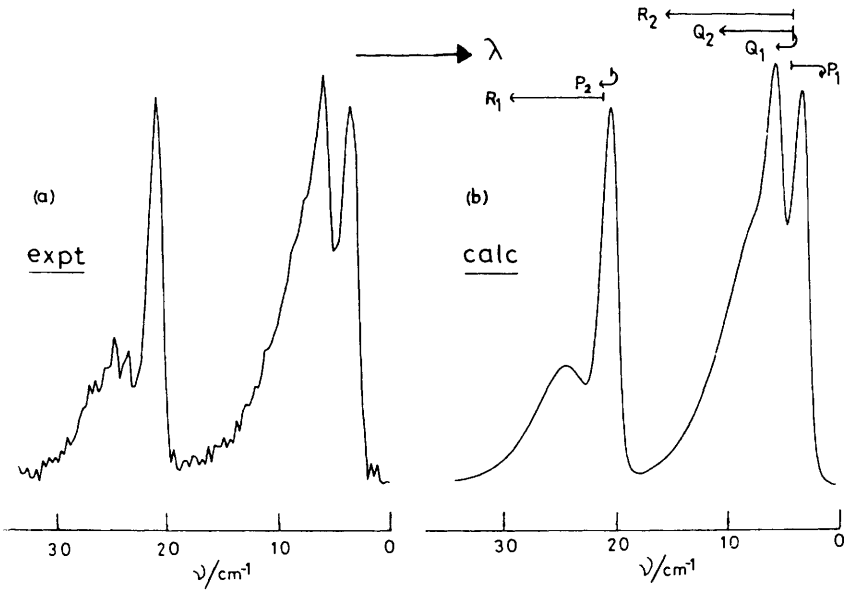

Figure 4 *(a) The* 1_2^0 *band of* CF_4^+ $\tilde{D}$—$\tilde{C}$ *at* 381 nm *recorded at a resolution of* 1.5 cm^{-1}. *(b) The best simulated spectrum; the six branches are marked*
(Reproduced by permission from *Mol. Phys.*, 1987, **62**, 184)

by the Jahn–Teller effect. The vibrational structure of the $\tilde{D}$—$\tilde{C}$ transition in these three fluorides indicates immediately that Jahn–Teller distortion is occurring in SiF_4^+ and GeF_4^+ $\tilde{C}\,^2T_2$ but not in CF_4^+ $\tilde{C}\,^2T_2$. Figure 3 shows the spectrum of CF_4^+ $\tilde{D}$—$\tilde{C}$ between 360—420 mm recorded at *ca.* 25K in the molecular beam apparatus. Only vibrational bands involving the ν_1 totally symmetric C—F stretching mode are observed, and the absence of bands involving the other three modes ν_2, ν_3, and ν_4 (of e, t_2, and t_2 symmetry respectively) shows that the $\tilde{C}$ state has tetrahedral symmetry and is not exhibiting Jahn–Teller distortion. Figure 4(a) shows the spectrum of the $v_1' = 0 \longrightarrow v_1'' = 2$ band at 381 nm recorded under much higher resolution. Figure 4(b) is a computer simulation of the rotational structure.[18] The agreement is excellent and confirms that this band is indeed due to a vibronic component of a $^2A_1$—$^2T_2$ transition in a tetrahedral molecule observed at a low rotational temperature. Several spectroscopic parameters (*e.g.* rotational constants and spin–orbit splitting constants) were deduced from this work. Recently, these bands in both CF_4^+ [19] and SiF_4^+ [20] have been photographed at Doppler-limited resolution (*ca.* 0.05 cm^{-1}), and when the analyses are complete these constants will be improved.

[18] S. M. Mason and R. P. Tuckett, *Mol. Phys.*, 1987, **62**, 175; S. M. Mason, Ph.D. Thesis, University of Cambridge, 1988.
[19] J. F. M. Aarts, personal communication.
[20] J. L. Chotin, S. Leach, I. R. Lambert, and R. P. Tuckett, unpublished data.

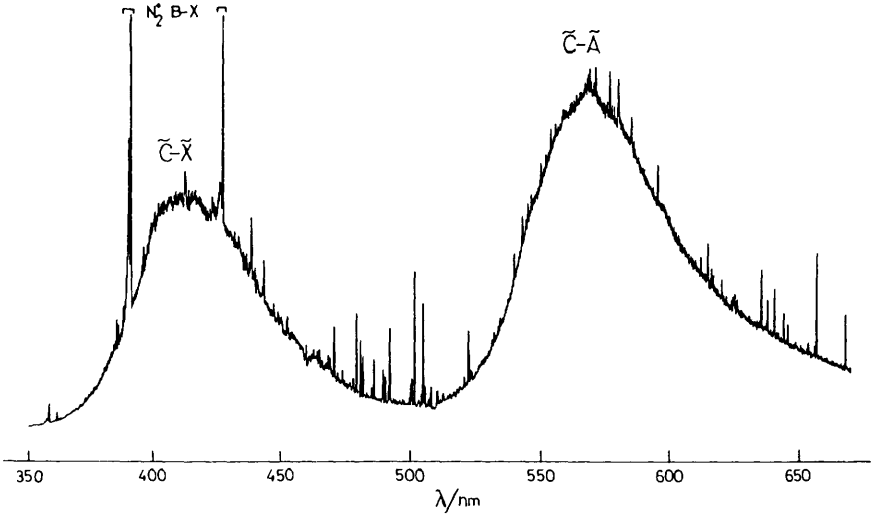

Figure 5 *Spectrum resulting from electron impact ionization of a* He-*seeded supersonic beam of* $SiCl_4$. *The two broad continuous bands are due to emission from* $SiCl_4^+$ $\tilde{C}\,^2T_2$ (Reproduced by permission from *J. Chem. Phys.*, 1988, **89**, 2678)

B. Bound–Free Continuous Spectra in MX_4^+.—Bound–free transitions are observed in CF_4^+ [21] and the tetrachloride and tetrabromide ions of silicon and germanium.[22,23] The $\tilde{C}\,^2T_2$ state of CF_4^+ decays radiatively by photon emission to the ground ($\tilde{X}\,^2T_1$) and first excited ($\tilde{A}\,^2T_2$) states, both of which are repulsive states in the Franck–Condon region. The $\tilde{C}$—$\tilde{A}$ and $\tilde{C}$—$\tilde{X}$ are electric dipole allowed transitions, so the spectrum appears as two (overlapping) structureless bands with peaks at 290 and 230 respectively. The four ions $SiCl_4^+$, $GeCl_4^+$, $SiBr_4^+$, and $GeBr_4^+$ all show radiative decay from the same $\tilde{C}\,^2T_2$ state to repulsive $\tilde{A}$ and $\tilde{X}$ states, and therefore two broad bands are observed in each emission spectrum; Figure 5 shows the spectrum of $SiCl_4^+$ $\tilde{C}$—$\tilde{X}$, $\tilde{A}$ resulting from electron impact ionization of a molecular beam of $SiCl_4$. The ions CCl_4^+ and CBr_4^+ do not fluoresce.

Spectroscopically, continuous spectra of this kind are of limited value. They do indicate that the upper electronic state is bound, and therefore can decay on the relatively slow timescale of photon emission (*ca.* 10^5—10^{10} s^{-1}). Also, because emission from the parent ion is proposed, it has to be shown that the wavelengths of the observed transitions are consistent with the separation of the electronic states of MX_4^+ as revealed by photoelectron spectroscopy. However, because detailed vibrational and rotational structure is not present, it is not

[21] J. F. M. Aarts, *Chem. Phys. Lett.*, 1985, **114**, 114.
[22] I. R. Lambert, S. M. Mason, R. P. Tuckett, and A. Hopkirk, *J. Chem. Phys.*, 1988, **89**, 2675.
[23] J. C. Creasey, I. R. Lambert, R. P. Tuckett, and A. Hopkirk, *J. Chem. Soc., Faraday Trans.*, 1990, **86**, 2021.

possible to assign an electronic spectrum on the basis of its high resolution spectroscopic features, as was possible with the CF_4^+ $\tilde{D}\,^2A_1$—$\tilde{C}\,^2T_2$ spectrum.[15] Thus assignments of bound–free spectra are always more uncertain.

C. Spectroscopic/Dynamics Experiments on MX_4^+.—These spectroscopic experiments served to highlight a number of new problems to be solved. Perhaps the first point to understand is why such fluorescence spectra are observed at all. Photon emission is being observed from excited electronic states of MX_4^+ which lie up to 10 eV above many dissociation channels (see Section 4). Whereas this behaviour would not be surprising for diatomic cations, with such sized five-atom polyatomics non-radiative processes would be expected to dominate. The observation of radiative decay is therefore very surprising. Some of the other questions to be answered are:

(a) For these states of MX_4^+ that decay by photon emission, what are the fluorescence quantum yields? Do they change when different parts of the potential energy surface are accessed?

(b) What are the radiative lifetimes of the fluorescing states, and again do they change with excitation energy?

(c) For a given central atom M, why do the fluorides behave differently from the chlorides and bromides, and for a given halide why does the carbon species behave differently from the silicon or germanium species?

(d) If the excited electronic state of MX_4^+ does not decay radiatively but (as expected) by a non-radiative process, what are the fragment ions produced and at what rate do these non-radiative processes occur?

(e) When the parent neutral molecule in the supersonic beam is excited with 200 eV non-resonant electrons, does fragmentation of MX_4 compete with ionization? Do the relative cross-sections for these processes change with energy?

(f) Perhaps most important of all, what if any is the relation between the spectroscopic and dynamic decay properties of these valence electronic states of MX_4^+? To take one example, CF_4^+ $\tilde{C}\,^2T_2$ does not show Jahn–Teller distortion from tetrahedral symmetry,[15] and this state decays radiatively. SiF_4^+ and GeF_4^+ $\tilde{C}$ do distort from T_d geometry,[16,17] but both states decay non-radiatively by loss of a fluorine atom to $SiF_3^+/GeF_3^+ + F$ (Section 5).[10] Does this imply that all excited electronic states of polyatomic ions that show Jahn–Teller distortion do not decay by photon emission, or is this a particular property of highly symmetrical tetrahedral species?

The pre-requisite to be able to address these problems is the ability to create a known flux of a particular electronic state of MX_4^+, ideally at vibrational resolution, in the absence of other species. This is most easily achieved with tunable vacuum UV photons from a synchrotron source and explains why we started experiments at Daresbury in 1987.

4 Experiments to Probe Radiative Decay of Excited Electronic States of Polyatomic Molecular Ions

We have used the apparatus described in Section 2 to probe radiative decay of

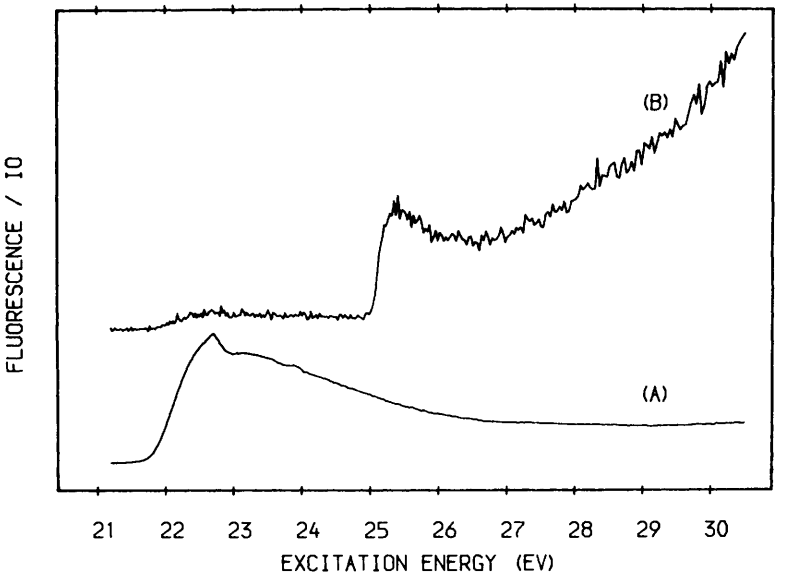

Figure 6 *Undispersed fluorescence of* CF_4 *excited by VUV photons in the range* 21—31 eV. *In* (*A*) *fluorescence in the range* 250—390 nm *is collected, in* (*B*) 120—200 nm *only is collected. The signals have been normalized to the synchrotron flux* I_0, *and the scale of this axis is different in the two spectra*
(Reproduced by permission from *J. Chem. Phys.*, 1988, **89**, 2685)

excited electronic states of polyatomic molecular ions, especially the group IV tetrahalide ions. This section reviews our results. It is divided into 'multi-bunch' fluorescence excitation experiments and 'single-bunch' lifetime measurements.

A. Multi-bunch (Quasi c.w.) Experiments.—(i) *The fluorides of Group IV.*[9] In these experiments we have used the tunable vacuum UV photon source to confirm what we already knew from our spectroscopic studies in Birmingham, that the singly-degenerate $\tilde{D}\,^2A_1$ state fluoresces in all three fluorides CF_4^+, SiF_4^+, and GeF_4^+ whereas only the triply-degenerate $\tilde{C}\,^2T_2$ state in CF_4^+ decays radiatively. Figure 6 shows the fluorescence excitation spectrum of CF_4 when excited by photons in the range 21—31 eV. In (A) an EMI 9883 QB photomultiplier tube is filtered so that only photons in the range 250—390 nm are collected; this encompasses most of the bound–free $\tilde{C}$—$\tilde{X}$ and $\tilde{C}$—$\tilde{A}$ transitions in CF_4^+. In (B) an EMI CsI 9413 solar blind tube (collecting $120 < \lambda < 200$ nm) is used; this encompasses most of the bound–free $\tilde{D}$—$\tilde{A}$ and $\tilde{D}$—$\tilde{B}$ transitions in CF_4^+. Thresholds are observed at 21.7 ± 0.1 and 25.0 ± 0.1 eV, in excellent agreement with the adiabatic ionization potentials (IP) of the $\tilde{C}$ and $\tilde{D}$ states of CF_4^+ (Table 1). These spectra show two important characteristics of a photoionization process. Firstly, the steepness of the 'turn-on' is governed by ionization Franck–Condon factors; Figure 6(B) shows a steep rise at threshold

Table 1 *Energetics of dissociation channels of* CF_4^+, SiF_4^+, CCl_4^+, *and* $SiCl_4^+$ *in* eV

Neutral/Parent Ion		*Dissociation Channel*	*Dissociation Energy*/eV	*Adiabatic IP*/eV
CF_4^+	$\tilde{D}\,^2A_1$			25.1
		$CF_2 + F_2^+$	23.2	
		$CF_3 + F^+$	22.9	
		$CF^+ + F + F_2$	22.1	
	$\tilde{C}\,^2T_2$			21.7
		$CF_2^+ + F + F$	20.8	
		$CF_2^+ + F_2$	19.2	
	$\tilde{B}\,^2E$			18.3
	$\tilde{A}\,^2T_2$			17.1
CF_4^+	$\tilde{X}\,^2T_1$			15.3
		$CF_3^+ + F$	14.7	
CF_4	$\tilde{X}\,^1A_1$			0
		$SiF_2 + F_2^+$	26.3	
		$SiF^+ + F + F_2$	24.6	
		$SiF_3 + F^+$	24.3	
		$SiF_2^+ + F + F$	23.0	
SiF_4^+	$\tilde{D}\,^2A_1$			21.5
		$SiF_2^+ + F_2$	21.4	
	$\tilde{C}\,^2T_2$			19.3
	$\tilde{B}\,^2E$			18.0
	$\tilde{A}\,^2T_2$			17.3
		$SiF_3^+ + F$	16.2	
SiF_4^+	$\tilde{X}\,^2T_1$			16.1
SiF_4	$\tilde{X}\,^1A_1$			0
CCl_4^+	$\tilde{D}\,^2A_1$			19.3
	$\tilde{C}\,^2T_2$			16.3
		$CCl^+ + Cl + Cl_2$	16.3	
		$CCl_3 + Cl^+$	16.0	
		$CCl_2^+ + Cl + Cl$	15.8	
		$CCl_2 + Cl_2^+$	15.0	
	$\tilde{B}\,^2E$			13.4
		$CCl_2^+ + Cl_2$	13.3	
	$\tilde{A}\,^2T_2$			12.3
		$CCl_3^+ + Cl$	11.8	
CCl_4^+	$\tilde{X}\,^2T_1$			11.5
CCl_4	$\tilde{X}\,^1A_1$			0
$SiCl_4^+$	$\tilde{D}\,^2A_1$			18.1
		$SiCl_3 + Cl^+$	17.8	
		$SiCl_2^+ + Cl + Cl$	17.7	
		$SiCl^+ + Cl + Cl_2$	16.8	
		$SiCl_2 + Cl_2^+$	16.6	
		$SiCl_2^+ + Cl_2$	15.2	

Table 1 *Continued*

Neutral/Parent Ion		*Dissociation Channel*	*Dissociation Energy*/eV	*Adiabatic IP*/eV
	$\tilde{C}\,^2T_2$			15 1
	$\tilde{B}\,^2E$			13 5
	$\tilde{A}\,^2T_2$			12 8
		$SiCl_3^+ + Cl$	12.7	
$SiCl_4^+$	$\tilde{X}\,^2T_1$			11 8
$SiCl_4$	$\tilde{X}\,^1A_1$			0

because ionization to $\tilde{D}\,^2A_1$ is a vertical process with very little change in molecular geometry, whereas the rise in Figure 6(A) is shallower because ionization to $\tilde{C}\,^2T_2$ involves a substantial change (0.08 Å) in the C—F bond distance.[18] Secondly, the fluorescence signal remains non-zero for photon energies well in excess of threshold. This is because photoionization is a non-resonant process since the electron can carry away the excess energy. The intensity of the emission is then determined primarily by the variation of the partial ionization cross-section for the ionic state in question with energy.

The EMI 9883 QB photomultiplier tube which detects CF_4^+ $\tilde{C}$—$\tilde{X}$,$\tilde{A}$ emission can also detect N_2^+ B—X (0,0) emission at 391 nm, and it has been possible to calibrate the photon collection efficiency of the apparatus with N_2^+. Since the partial ionization cross-section into CF_4^+ $\tilde{C}$ is known as a function of energy from angle-resolved photoelectron spectroscopy,[24] it is possible to estimate the fluorescence quantum yield of CF_4^+ $\tilde{C}$. The procedure is described elsewhere.[9] We obtain $\Phi_{h\nu} = 0.5 \pm 0.4$, suggesting that a competing non-radiative channel is operative (see Section 5). Measurements of fluorescence quantum yields by this method are rare, since partial ionization cross-sections are only known for relatively few of the polyatomic molecules we have studied, and the photomultiplier tube used has to be sensitive at 391 nm to calibrate with N_2^+ B—X. For this latter reason it was not possible to estimate $\Phi_{h\nu}$ for the $\tilde{D}$ state of CF_4^+.

(ii) *The Chlorides and Bromides of Group IV.*[22,23] In these experiments we used the tunable vacuum UV radiation to show that the bound–free broad bands seen in the electron impact spectra (Section 3.B) are related to the initial formation of the $\tilde{C}\,^2T_2$ state of the parent molecular ion. Figure 7 shows the fluorescence excitation spectrum of $SiCl_4$ excited with photons in the range 14—35 eV. Only fluorescence in the range 320—470 nm was collected, corresponding to the lower wavelength band in Figure 5. An identical excitation spectrum was obtained when fluorescence in the range 505—705 nm was collected, corresponding to the higher wavelength band in Figure 5. Therefore the two emission bands have the same upper state. The two characteristics of a photoionization process described in Section 4.A(i) are observed, and the threshold appears at 15.1 ± 0.1 eV. This corresponds to the adiabatic IP of the $\tilde{C}\,^2T_2$ state of $SiCl_4^+$ [25] and therefore the

[24] T A Carlson, A Fahlman, W A Svensson, M O Krause, T A Whitley, F A Grimm, M N Piancastelli, and J W Taylor, *J Chem Phys*, 1984, **81**, 3828

[25] P J Bassett and D R Lloyd, *J Chem Soc A*, 1971, 641

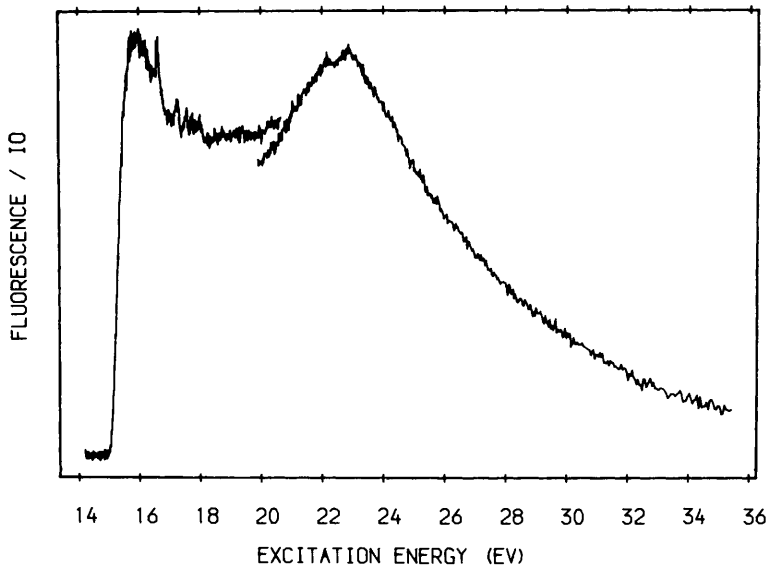

Figure 7 *Undispersed fluorescence of* $SiCl_4$ *excited by VUV photons in the range* 14—35 eV. *Only photons in the range* 320—470 nm *are collected, and the signal has been normalized to the synchrotron flux* I_0
(Reproduced by permission from *J. Chem. Phys.*, 1988, **89**, 2679)

emission is related to the initial formation of $SiCl_4^+$ $\tilde{C}$. The excellent agreement of the wavelengths of the emissions with predictions from photoelectron data for $SiCl_4$[22] suggests very strongly that the two bands are due to $SiCl_4^+$ $\tilde{C}$—$\tilde{X}$ and $\tilde{C}$—$\tilde{A}$. Partial ionization cross-section data are available for $SiCl_4$,[26] and we used them to estimate the fluorescence quantum yield of $SiCl_4^+$ $\tilde{C}$ to be 0.2—0.4. The lifetime data (Section 4.B), however, suggest that radiative decay is the only channel operative and therefore $\Phi_{h\nu}$ should be unity.

Very similar fluorescence excitation spectra were obtained with $GeCl_4$, $SiBr_4$, and $GeBr_4$. In all cases the two fluorescence bands observed in the electron impact spectrum can be assigned to parent ion emission from (the bound) $\tilde{C}\ ^2T_2$ state to lower-lying (repulsive) $\tilde{X}\ ^2T_1$ and $\tilde{A}\ ^2T_2$ states. Partial ionization cross-section data are not available, so it has not been possible to estimate $\Phi_{h\nu}$ for these states. However, like $SiCl_4^+$ $\tilde{C}$ they are believed to have the maximum value of unity.

(iii) *The Mixed Halides of Group IV.*[27] In order to establish whether the observation of radiative decay from excited states of the tetrahedral ions MX_4^+ was due to their high degree of molecular symmetry, we studied halides of group

[26] T. A. Carlson, A. Fahlman, M. O. Krause, T. A. Whitley, F. A. Grimm, M. W. Piancastelli, and J. W. Taylor, *J. Chem. Phys.*, 1986, **84**, 641.
[27] J. C. Creasey, I. R. Lambert, R. P. Tuckett, and A. Hopkirk, *Mol. Phys.*; two papers in press.

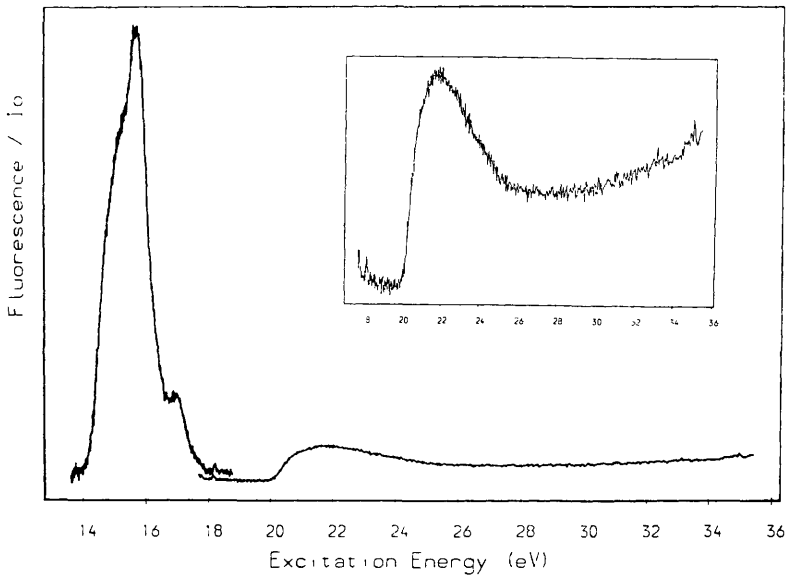

Figure 8 *Undispersed fluorescence of* CF_3H *excited by VUV photons in the range* 13.5—35.5 eV. *Only photons in the range* 230—400 nm *are collected, and the signal has been normalized to the synchrotron flux* I_0

IV of lower symmetry. Four molecules were studied, CF_3H, CF_3Cl, and $CFCl_3$ (of C_{3v} symmetry) and CF_2Cl_2 (of C_{2v} symmetry), first in the electron beam apparatus at Birmingham and then in the fluorescence excitation apparatus at Daresbury. Parent ion emission is observed in CF_3H^+ and CF_3Cl^+ but not in the other two molecules. Figure 8 shows the fluorescence excitation spectrum of CF_3H excited with vacuum UV photons in the range 13.5—35.5 eV, fluorescence being collected in the range 230—400 nm. Two quite different features are observed. The peaks between 14 and 18 eV are resonant peaks and are due to CF_2 $\tilde{A}$—$\tilde{X}$ fluorescence following excitation of dissociative Rydberg states of CF_3H. The shape of this feature is characteristic of a neutral excitation process where the photon energy scans through the Franck–Condon region of the dissociative Rydberg states. Thus the excitation spectrum shows a slow increase from threshold, reaches a peak, and recedes to the baseline. Because this is a resonant process, these states cannot be populated by higher energy photons. The much weaker feature with threshold at 20 eV, however, is due to a primary photoionization process [see Section 4.A(i)] and the fluorescing state of CF_3H^+ is the (bound) $\tilde{D}\,^2A_1$ state with a vertical ionization potential of 20.5 eV. Emission is to lower electronic states of CF_3H^+ which may be bound or repulsive.

This spectrum highlights particularly well one of the advantages of using photons over electrons as a method for ionization. Using 200 eV electrons in the molecular beam apparatus, the dispersed fluorescence spectrum from CF_3H

between 230 and 400 nm is dominated by CF_2 $\tilde{A}$—$\tilde{X}$ emission,[27] since the much weaker bands due to CF_3H^+ in this region are swamped. The second advantage is that thresholds for both resonant dissociative and non-resonant ionization processes are much more accurately determined with photons than with electrons. For an ionization process, this is because with photon excitation the cross-section usually shows a step function at threshold, whereas with electrons the cross-section increases only slowly and linearly with the excess energy above threshold.[28] Establishing the threshold in the latter case can therefore be difficult, and there are many inaccurate values in the literature over the past twenty years just because this point has not been appreciated. This has often led to over-interpretation and incorrect assignments.

The fluorescence excitation spectra of CF_3Cl, CF_2Cl_2, and $CFCl_3$ all show resonant features in the 10—19 eV range, fluorescence being due to excited states of the fragments CF_3, CF_2, and CF. Full details can be found elsewhere.[27] Like CF_3H, CF_3Cl shows parent ion emission from a bound state at higher photon energy, the fluorescing state being the $\tilde{E}\,^2A_1$ state of CF_3Cl^+ with a vertical ionization potential of 20.2 eV. Parent ion emission could not be detected from any valence ionic state of $CF_2Cl_2^+$ or $CFCl_3^+$.

(iv) *The Halides of Group III.* We have just initiated a study of fluorescence processes following vacuum UV photoexcitation or electron excitation of the halides of group III (see ref. 35). We wish to determine whether the (surprising) observation of radiative decay from highly excited valence states of the group IV halides is a property of group IV species, or whether it is a general property of similar-sized molecules. In this paper we report preliminary results on BF_3 and BCl_3, two halides of group III of D_{3h} symmetry. In the tetrahedral ions MX_4^+, the states from which radiative decay is observed ($\tilde{C}\,^2T_2$ and $\tilde{D}\,^2A_1$) arise from electron removal from σ-bonding molecular orbitals in neutral MX_4, whereas the lower electronic states of the ion ($\tilde{X}\,^2T_1$, $\tilde{A}\,^2T_2$, and $\tilde{B}\,^2E$) arise from electron removal from halogen $p\pi$ non-bonding orbitals.[29] In both BF_3 and BCl_3, simple MNDO calculations show that the same pattern of molecular orbitals is observed. The first four HOMOs (electron removal from which give the $\tilde{X}\,^2A_2'$, $\tilde{A}\,^2E'$, $\tilde{B}\,^2E''$, and $\tilde{C}\,^2A_2''$ states of the ion) are predominantly halogen non-bonding orbitals, whereas the next two orbitals (electron removal from which give $\tilde{D}\,^2E'$ and $\tilde{E}\,^2A_1'$) are σ-bonding between boron 2*s* or 2*p* and the halogen *np*σ atomic orbitals. If the same pattern is observed, it is therefore from the $\tilde{D}$ or $\tilde{E}$ states of BF_3^+ and BCl_3^+ that we might expect to observe radiative decay. These states have adiabatic energies of 621 and 576 Å in BF_3^+,[30,31] 809 and 699 Å in BCl_3^+,[30] so are suitable for study using the high energy grating of the Seya monochromator.

Both molecules show resonant dissociative peaks at high photon wavelengths

[28] G. H. Wannier, *Phys. Rev.*, 1953, **90**, 817.
[29] R. N. Dixon and R. P. Tuckett, *Chem. Phys. Lett.*, 1987, **140**, 553.
[30] P. J. Bassett and D. R. Lloyd, *J. Chem. Soc., A*, 1971, 1551.
[31] L. Asbrink, A. Svensson, W. von Niessen, and G. Bieri, *J. Elec. Spectrosc.*, 1981, **24**, 293.

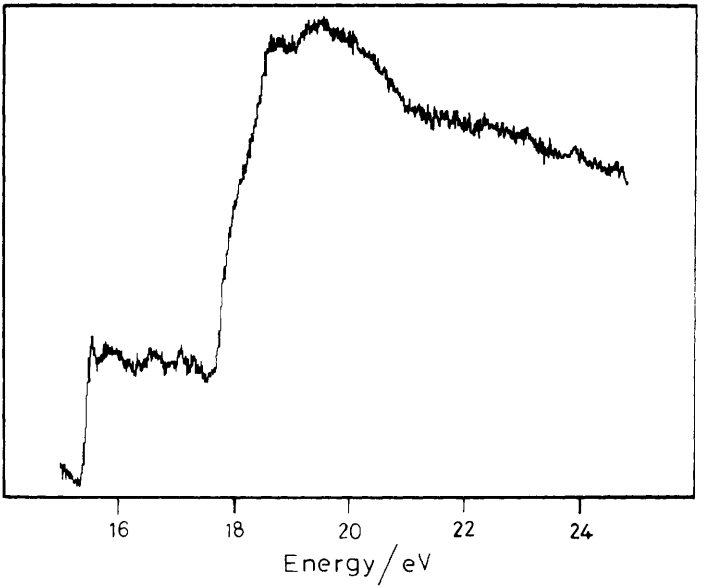

Figure 9 *Undispersed fluorescence of* BCl_3 *excited by VUV photons in the range* 15—25 eV. *Only photons in the range* 300—550 nm *are collected, and the signal has been normalized to the synchrotron flux* I_0

($\lambda > 850$ Å) and non-resonant ionization peaks at lower wavelengths. BCl_3 has been studied previously by Lee *et al.*[32] both above and below the lithium fluoride cut-off. Resonant peaks between 1050 and 1250 Å were assigned to BCl_2 emission, at 920 Å to BCl A—X emission, and we observe these same features. Lee *et al.* assign a sharp threshold at 810 Å in the fluorescence excitation spectrum to emission from the $\tilde{D}\,^2E'$ state of BCl_3^+, and they also believe the $\tilde{C}\,^2A_2''$ state fluoresces weakly. Whereas our spectra are similar in the region of the resonant dissociative peaks, our excitation spectra at lower wavelengths are rather different. Figure 9 shows our spectrum of BCl_3 excited in the range 15—25 eV, fluorescence being observed between 300 and 550 nm. Steep rises are observed at 15.3 eV (810 Å) and 17.6 eV (705 Å), and we assign these to emission from the $\tilde{D}\,^2E'$ and $\tilde{E}\,^2A_1'$ states of BCl_3^+ respectively. Similar spectra are obtained when the filter is replaced by a different cut-on filter transmitting $\lambda > 420$ nm, and by a UV filter transmitting 230—400 nm. Thus both $\tilde{D}$ and $\tilde{E}$ state fluorescence is occurring over a wide range of the UV/visible, and this is compatible with the wavelengths of allowed electronic transitions in BCl_3^+ predicted from photoelectron spectroscopy. We see no evidence for emission from the $\tilde{C}\,^2A_2''$ state.

VUV photoexcitation of BF_3 has not been studied before. Figure 10 shows the fluorescence excitation spectrum between 11.3 and 17.7 eV with fluorescence

[32] M Suto, C Ye, J C Han, and L C Lee, *J Chem Phys*, 1988, **89**, 6653, L C Lee, J C Han, and M Suto, *J Chem Phys*, 1989, **91**, 2036

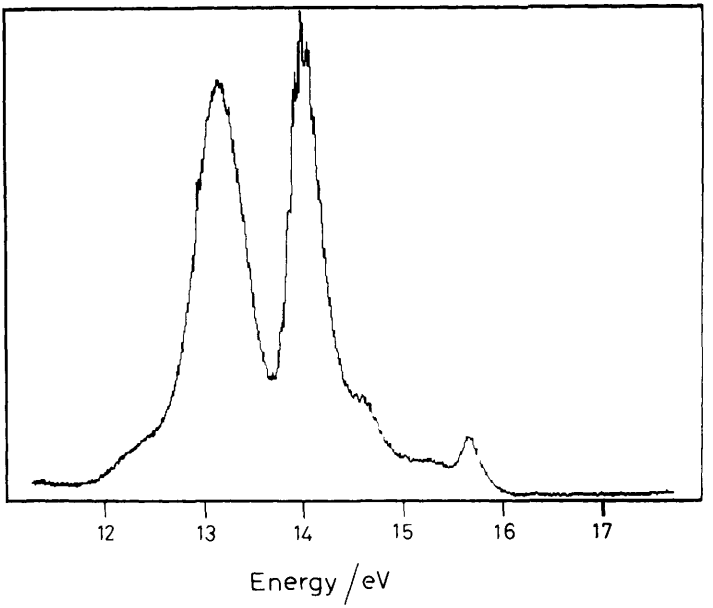

Figure 10 *Undispersed fluorescence of* BF_3 *excited by VUV photons in the range* 11.3—17.7 eV. *Only photons in the range* 230—400 nm *are collected, and the signal has been normalized to the synchrotron flux* I_0

collected between 230 and 400 nm. The two strong resonant peaks at 13.1 and 14.0 eV show very different relative intensities when filters isolating different parts of the 230—400 nm region are used. They also have different radiative lifetimes (Section 4.B). By analogy with BCl_3, we assign these peaks to BF_2 emission, fluorescence emanating from two close-lying excited electronic states of this radical. Emission is probably to its ground state. Surprisingly, there are no experimental or theoretical data on this 17-electron triatomic free radical, and we hope this work will stimulate *ab initio* potential energy surface calculations. We comment that BF_2 is isoelectronic with FCO, and although a gas phase electronic spectrum of FCO has not categorically been observed, Jacox[33] has observed two close-lying UV electronic transitions of FCO in an argon matrix. The bands we observe in BF_2 may be analogous to these two transitions. Figure 11 shows the excitation spectrum of BF_3 in the range 18—28 eV. The steep rise at 21.5 eV (576 Å) is assigned to emission from the $\tilde{E}\,^2A_1'$ state of BF_3^+. The use of different filters shows that emission is predominantly in the UV below 300 nm, and this is compatible with predictions from photoelectron spectroscopy. There is no evidence for emission from the $\tilde{D}$ or $\tilde{C}$ states of BF_3^+ at 20.0 eV (621 Å) and 18.9 eV (655 Å) respectively.

(v) *Non-fluorescing Halides of Groups III—VI.* Of all the halides of groups III,

[33] M. E. Jacox, *J. Mol. Spectrosc.*, 1980, **80**, 257.

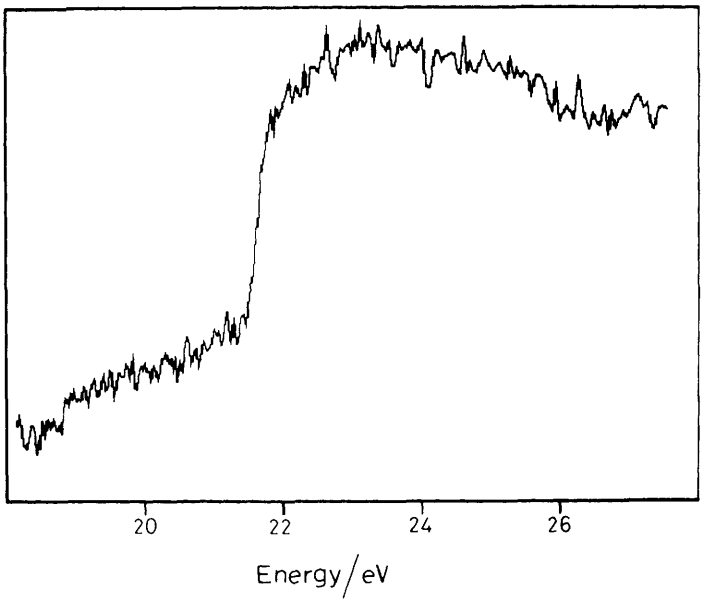

Figure 11 *Undispersed fluorescence of* BF_3 *excited by VUV photons in the range* 18–28 eV *Photons in the range* 230—400 nm *are collected and the signal has been normalized to the synchrotron flux* I_0

IV, and VI which have been studied, radiative decay has not been observed from excited electronic states of CCl_4^+, CBr_4^+, and SF_6^+ We estimate that, given a favourable partial ionization cross-section, it should be possible to detect radiative decay from an electronic state with fluorescence quantum yield greater than *ca* 10^{-3} in our apparatus This means that for these states of CCl_4^+, CBr_4^+, and SF_6^+ non-radiative decay (*e g* by fragmentation) is occurring at least one thousand times faster than any radiative decay process

B. Single-bunch (Pulsed) Experiments.—Radiative lifetimes were measured using the single-bunch mode of the synchrotron source The pulse width is *ca* 200 ps, the flight time around the ring 320 ns, and this is a superb source for measuring radiative lifetimes in the range 1—100 ns with a high degree of precision Lifetimes outside this range (especially smaller values) can be measured, but careful deconvolution techniques for the excitation pulse need to be employed Data accumulate rapidly due to the high repetition rate (3 MHz) of the source, so these experiments can be performed very quickly Results are shown in Tables 2 and 3 Table 2 gives the lifetimes of fluorescing states of parent molecular ions, whereas Table 3 gives values for neutral fragments formed by resonant photodissociation of a Rydberg state of the parent neutral molecule [Sections 4 A(iii) and 4 A(iv)]

For strong fluorescing states of parent ions, lifetimes τ were measured at

Table 2 *Radiative lifetimes of fluorescing states of polyatomic molecular ions studied in this work*

Ion	*Electronic State*	*Adiabatic IP*/eV	τ/ns	*Ref.*
CF_4^+	$\tilde{D}\,^2A_1$	25.1	2.1	34
	$\tilde{C}\,^2T_2$	21.7	9.7—8.6	9
SiF_4^+	$\tilde{D}\,^2A_1$	21.5	9.3	9
GeF_4^+	$\tilde{D}\,^2A_1$	21.3	3.1 and 6.3	9
$SiCl_4^+$	$\tilde{C}\,^2T_2$	15.1	38.4	9
$GeCl_4^+$	$\tilde{C}\,^2T_2$	14.6	65.4	9
$SiBr_4^+$	$\tilde{C}\,^2T_2$	13.8	47.6	23
$GeBr_4^+$	$\tilde{C}\,^2T_2$	13.4	67.1	23
CF_3H^+	$\tilde{D}\,^2A_1$	20.0	82	27
CF_3Cl^+	$\tilde{E}\,^2A_1$	19.9	27	27
BF_3^+	$\tilde{E}\,^2A_1'$	21.5	11.8	35
BCl_3^+	$\tilde{E}\,^2A_1'$	17.7	17.3	35
BCl_3^+	$\tilde{D}\,^2E'$	15.3	13.8	35

Table 3 *Radiative lifetime of fluorescing states of neutral fragments studied in this work*

Precursor Molecule	*Excitation Energy*/eV	*Fluorescence Collection Region*/nm	τ/ns	*Assignment*	*Ref.*
CF_3H	11.7	200—400	17.3	CF_3 UV band	27
	11.7	400—560	17.5	CF_3 visible band	27
	15.7	230—400	51.8	$CF_2\ \tilde{A}\,^1B_1$	27
CF_3Cl	15.9	230—400	46.3	$CF_2\ \tilde{A}\,^1B_1$	27
CF_2Cl_2	13.0	230—400	47.7	$CF_2\ \tilde{A}\,^1B_1$	27
	19.4	230—400	26.8	$CF\ A\,^2\Sigma^+$	27
BF_3	13.1	230—400	47.5	BF_2 UV band 1	35
	14.0	230—400	16.1	BF_2 UV band 2	35
BCl_3	10.7	230—400	26.2	BCl_2	35
	10.7	420—560	24.0	BCl_2	35

several excitation energies above threshold. Since $\tau^{-1} = k_{rad} + k_{non\text{-}rad}$, these experiments were performed because a change in τ would indicate the presence or even onset of a competing non-radiative decay channel of that electronic state. Thus lifetimes were measured as a function of energy for CF_4^+ $\tilde{C}$, SiF_4^+ $\tilde{D}$,

[34] J. E. Hesser and K. Dressler, *J. Chem. Phys.*, 1967, **47**, 3443.
[35] J. C. Creasey, I. R. Lambert and R. P. Tuckett, in preparation.

$SiCl_4^+$ $\tilde{C}$, $GeCl_4^+$ $\tilde{C}$, and $SiBr_4^+$ $\tilde{C}$. In the other cases the weakness of the signal and/or the limited time available at the SRS for single-bunch experiments precluded these measurements. Surprisingly and rather disappointingly, only in the case of CF_4^+ $\tilde{C}$ were we able to observe a change of τ with energy,[9] and even then the change is small (Table 2); the lifetime decreases from 9.7 ns just above threshold to a minimum of 8.6 ns at *ca.* 4 eV above threshold. This result suggests that a non-radiative channel is competing weakly with radiative decay, and this is compatible with the non-unity fluorescence quantum yield for this state of 0.5 ± 0.4 [Section 4.A(i)]. In fact this channel is fragmentation to CF_2^+ + F_2 or (F + F) (Section 5), and it is occurring at a relatively slow rate so that radiative decay can be observed with reasonable sensitivity. For the other four ionic states mentioned above, no variation of τ with energy is observed. This strongly implies that no non-radiative channel is competing with fluorescence, and therefore $\Phi_{h\nu}$ has its maximum value of unity in all four cases. The large values of the lifetimes (especially for the chlorides and bromides) appear to confirm this.

There are several extra comments to make about the data in Tables 2 and 3:

(a) For the other parent ions, lifetimes were measured at the peak of the excitation spectrum [*e.g.* that of BF_3^+ $\tilde{E}$ was measured at 23.2 eV (Figure 11)].

(b) We now believe that the bi-exponential decay observed[9] in GeF_4^+ $\tilde{D}$ is an artefact of how the electronics were set up for that particular measurement. In no other cases are anything other than single exponential decays observed.

(c) There is some controversy about the electronic spectroscopy of CF_3. Suto and Lee[36] believe that the two emission bands in the UV and visible emanate from different electronic states, whereas our lifetime data seem to suggest that only one state is involved in radiative decay.

(d) The lifetime of CF_2 $\tilde{A}$ has been measured by several workers in totally different experiments, and our value of *ca.* 50 ns is in excellent agreement.

(e) Our value for the CF $A\,^2\Sigma^+$ state lifetime agrees well with that of a recent measurement by Booth and Hancock,[37] and disagrees with the earlier accepted value of *ca.* 19 ns.

(f) The very different lifetimes of the two strong resonant peaks in BF_3 suggest that two fluorescing states of the fragment are being formed. BF_2 seems the most likely candidate, and *ab initio* calculations of the energies of the ground and excited electronic states, electronic transition moments, and radiative lifetimes would be most timely.

5 Experiments to Probe Non-radiative Decay of Excited Electronic States of Polyatomic Molecular Ions

We have used the coincidence apparatus described in Section 2 to probe the non-radiative decay channels of electronic states of the group IV tetrahalide ions. We are especially interested in those excited states which do not decay by photon

[36] M. Suto and L. C. Lee, *J. Chem. Phys.*, 1983, **79**, 1127.
[37] J. P. Booth and G. Hancock, *Chem. Phys. Lett.*, 1988, **150**, 457.

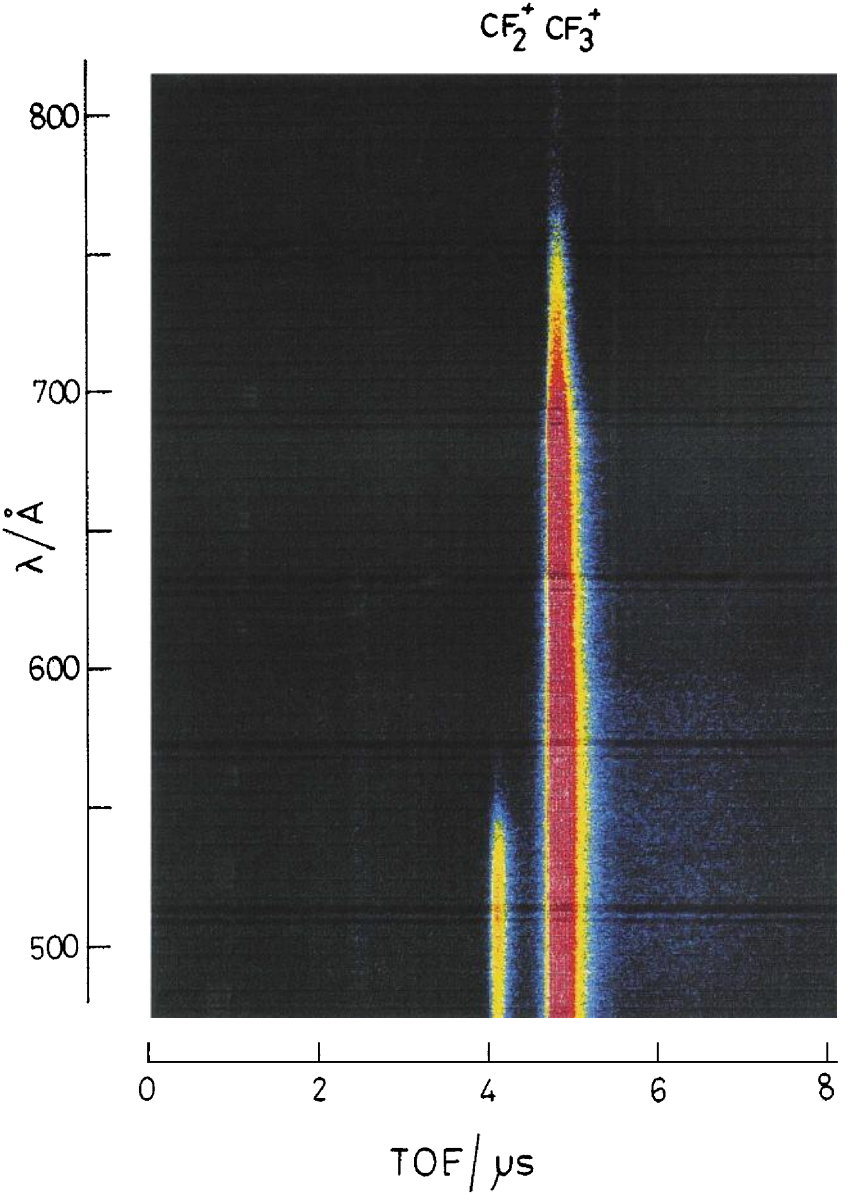
CF_2^+ CF_3^+
800
700
600
500
λ/Å
0
2
4
6
8
TOF/μs

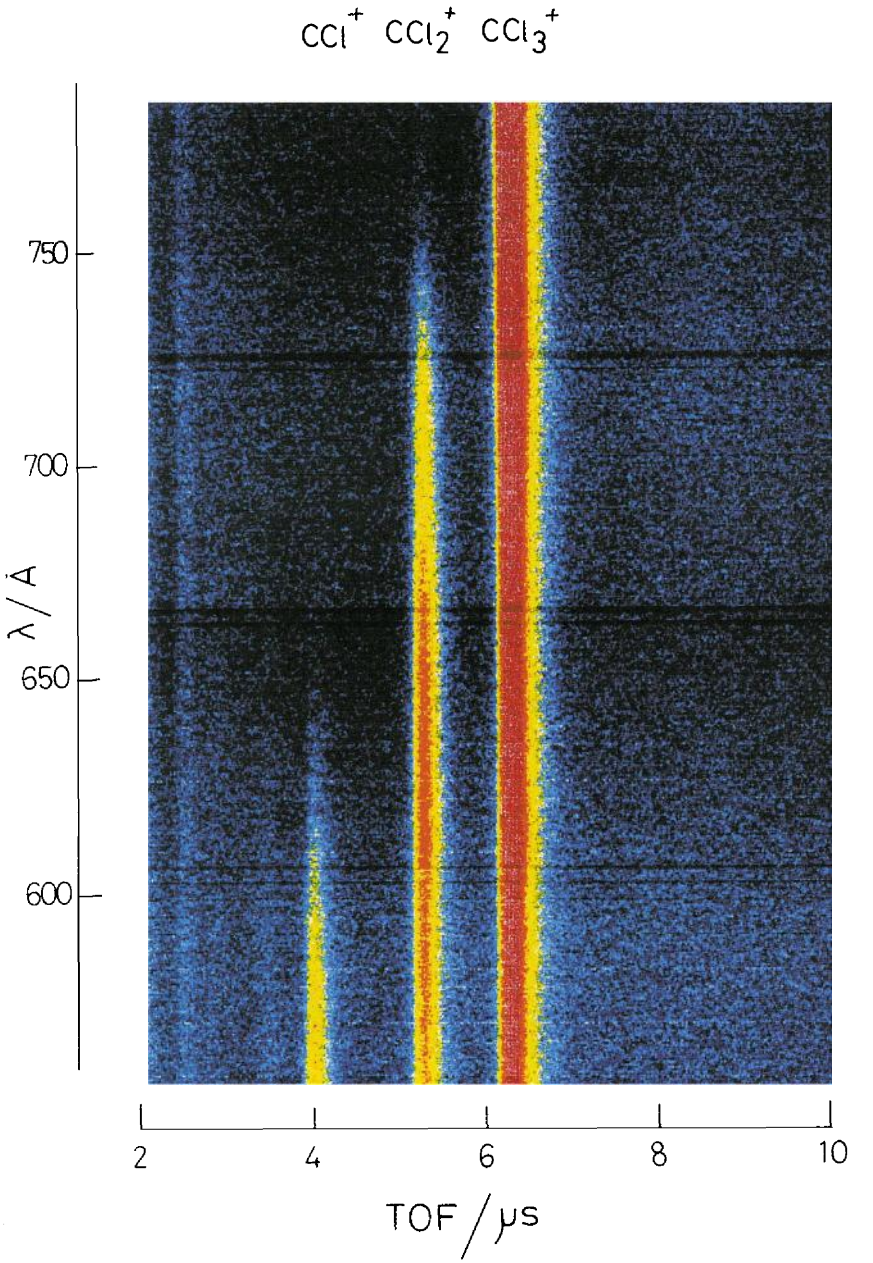
CCl^+ CCl_2^+ CCl_3^+
750
700
650
600
λ / Å
2
4
6
8
10
TOF / μs

emission or have a fluorescence quantum yield which is less than unity, since a non-radiative channel must then be operative. To date, we have made an extensive study of fragmentation of CF_4^+, SiF_4^+, CCl_4^+, $SiCl_4^+$ and $GeCl_4^+$ (ref. 10), $SiBr_4^+$ and $GeBr_4^+$ (ref. 38), and SF_6^+ (ref. 39). Data have not been obtained for GeF_4^+ and CBr_4^+, in the former case because GeF_4 was found to poison the microchannel plates, in the latter case because CBr_4 has too low a vapour pressure. We have unanalysed data for CF_3H^+, but have not yet studied the three chlorofluorocarbon ions CF_3Cl^+, $CF_2Cl_2^+$, and $CFCl_3^+$ because they have been studied in a more conventional PIMS apparatus elsewhere.[40]

Since this work involves the formation of fragment ions, we need to know the energies of the different ionic fragmentation channels. Values are given in Table 1 for the possible channels from CF_4^+, SiF_4^+, CCl_4^+, and $SiCl_4^+$ up to *ca.* 25 eV. These thermodynamic energies are calculated from heats of formation of the neutrals and ionization potentials of the fragments. Full details and the sources of the data are given elsewhere.[9,22] Two points should be made. Firstly, it should be noted that several dissociation channels are energetically open to the $\tilde{C}$ and $\tilde{D}$ states of MX_4^+, so observation of radiative decay from these states is a surprising phenomenon. For example, CF_4^+ $\tilde{C}\,^2T_2$ lies above channels dissociating to CF_3^+ and CF_2^+, yet this state fluoresces admittedly with a quantum yield which is less than unity [Section 4.A(i)]. Its $\tilde{D}\,^2A_1$ state at 25.1 eV has six different ionic channels open to it, yet it fluoresces strongly almost certainly with a quantum yield of unity. Secondly, the fluorides and chlorides behave very differently. For example, the $\tilde{D}\,^2A_1$ state of CCl_4^+ has the same equivalent six dissociation channels open that are open to CF_4^+ $\tilde{D}\,^2A_1$, yet it decays as one might expect non-radiatively to one or more of these channels. Thermodynamic data for the two bromides studied and SF_6^+ can be found in the respective papers.[23,39]

A. Fragmentation of the Fluorides of Group IV.[10]—Non-radiative decay of CF_4 and SiF_4 excited by vacuum UV radiation was studied from below the energy of the $\tilde{X}\,^2T_1$ ionic state to above that of the highest valence ionic state $\tilde{D}\,^2A_1$. Thus for CF_4, the range 480—820 Å was covered in six wavelength scans of *ca.* 70 Å, each with a small overlap between scans. The colour three-dimensional map incorporating all the scans 'spliced' together is shown in Figure 12 (see opposite p. 460). Only two ion peaks are observed, CF_2^+ for $\lambda < 572$ Å and CF_3^+ for $\lambda < 785$ Å, and the ion yield curves as a function of photon wavelength are shown in Figures 13 and 14. Two thresholds are apparent for CF_3^+ production at 785 Å (15.8 eV) and 720 Å (17.2 eV), and these correspond to the adiabatic energies of the $\tilde{X}$ and $\tilde{A}$ states of CF_4^+. CF_4^+ does *not* turn on at its thermodynamic energy of 14.7 eV or 843 Å. Similarly a threshold for CF_2^+ production is observed at 572 Å (21.7 eV) which is the adiabatic IP of the $\tilde{C}\,^2T_2$ state of CF_4^+. Again CF_2^+ does

[38] J. C. Creasey, I. R. Lambert, R. P. Tuckett, K. Codling, L. J. Frasinski, P. A. Hatherly, and M. Stankiewicz, unpublished data.

[39] J. C. Creasey, I. R. Lambert, R. P. Tuckett, K. Codling, L. J. Frasinski, P. A. Hatherly, M. Stankiewicz, and D. M. P. Holland, *J. Chem. Soc., Faraday Trans.*, submitted.

[40] H. W. Jochims, W. Lohr, and H. Baumgartel, *Ber. Bunsenges. Phys. Chem.*, 1976, **80**, 130.

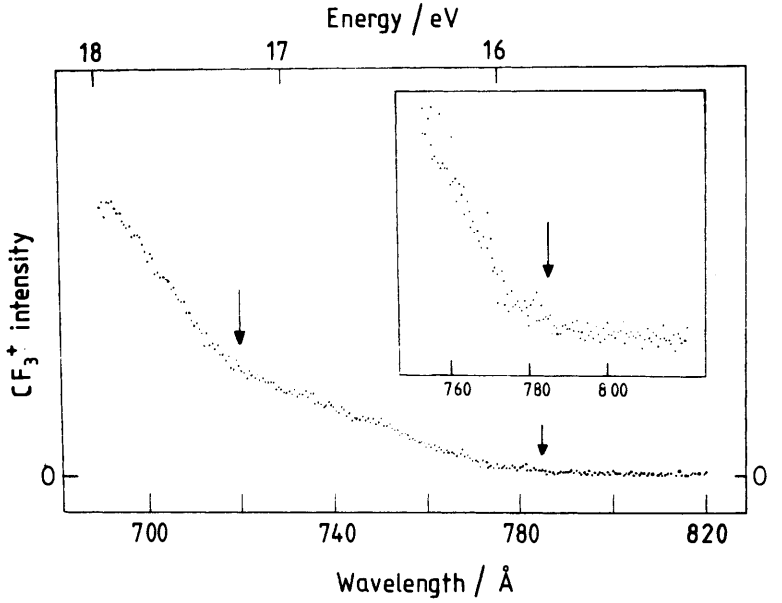

Figure 13 *Photoionization yield curve of* CF_3^+ *from* CF_4 *in the range* 690—820 Å. *The two thresholds for* CF_3^+ *production are marked*
(Reproduced by permission from *J. Chem. Phys.*, 1990, **93**, 3299.)

not turn on at the lowest thermodynamic channel forming CF_2^+ of 19.2 eV or 645 Å. It is important to appreciate that this is the opposite of what is usually observed with polyatomic molecular ions (*e.g.* CH_4^+ [41]), where the fragment ions appear at their thermodynamic threshold. This is almost certainly due to the totally repulsive nature of the ground state of CF_4^+. This state dissociates promptly to $CF_3^+ + F$, and dissociation of high vibrational levels of CF_4^+ $\tilde{X}$ is not a route for fragment ion production.

This work shows that the non-radiative decay channel of CF_4^+ $\tilde{C}$ which competes with radiative decay is fragmentation to CF_2^+. It is not easy to say whether the other product is F_2 or F + F. In principle this should be possible because the former channel involves a KE release of 2.5 eV at threshold, the latter only 0.9 eV (Table 1), and the width of the CF_2^+ ion peak in the TOF spectrum is related to the KE release. In practice it is not so simple [10] because many different vibrational levels of CF_4^+ $\tilde{C}$ contribute to the KE release when the photon energy exceeds threshold, and the available energy may also be channelled into vibration and rotation of the molecular fragments. The fact that fragmentation is slow enough that fluorescence can compete does perhaps suggest that one of the products involves the formation of a new chemical bond

[41] O. Dutuit, M. Alt-Kaci, J. Lemaire, and M. Richard-Viard, *Phys. Scr.*, 1990, **T31**, 223: Ref. 12, p. 274.

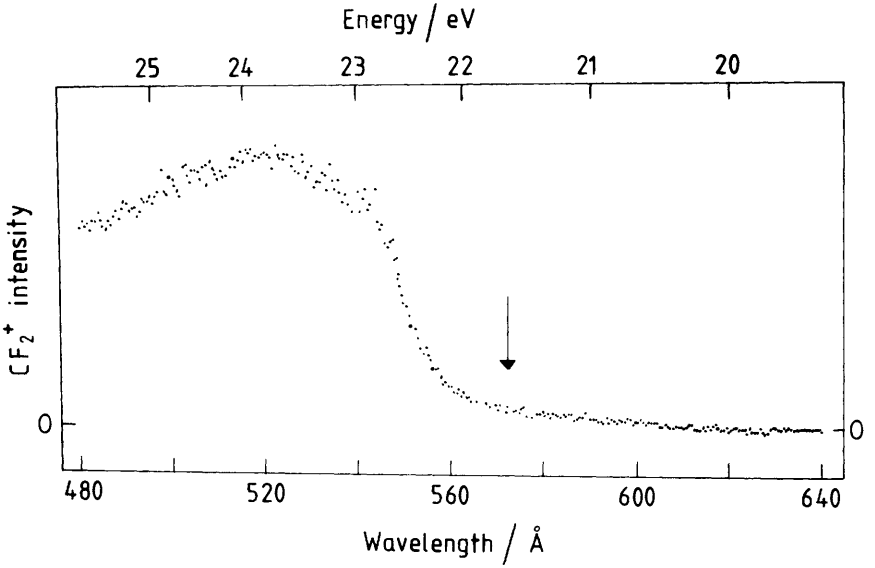

Figure 14 *Photoionization yield of* CF_2^+ *from* CF_4 *in the range* 480—640 Å. *The threshold for* CF_2^+ *production is marked*
(Reproduced by permission from *J. Chem. Phys.*, 1990, **93**, 3299)

(*i.e.* $CF_2^+ + F_2$). As mentioned in Section 2, accurate interpretation of KE releases in this form of experiment needs the internal energy of the parent ion to be defined uniquely, and this is most easily accomplished using a threshold electron detector. No new thresholds are observed for CF_3^+, CF_2^+, or any other ion at the CF_4^+ $\tilde{D}$ state adiabatic energy of 493 Å (25.1 eV), and this is confirming evidence that this state decays only by photon emission.

With SiF_4 only SiF_3^+ and SiF_4^+ are observed in the photon range studied (550—775 Å). Despite being energetically accessible SiF_2^+ is not observed. The SiF_4^+ ion yield curve shows a threshold at the adiabatic energy of the $\tilde{X}\,^2T_1$ state (770 Å or 16.1 eV), as expected. The SiF_3^+ curve (Figure 15) shows thresholds at 763 Å (16.2 eV) and 718 Å (17.3 eV). The former is the thermodynamic energy of the $SiF_3^+ +$ F channel, the latter the adiabatic energy of SiF_4^+ $\tilde{A}\,^2T_2$. This result can be explained as follows. Unlike CF_4^+, the ground state of SiF_4^+ does have a minimum in some part of its multi-dimensional potential energy surface, and therefore production of SiF_3^+ *via* dissociation of excited vibrational levels of SiF_4^+ $\tilde{X}$ is the lowest energy route. SiF_4^+ $\tilde{A}$ however is totally repulsive, dissociating promptly by loss of a fluorine atom to $SiF_3^+ +$ F, and therefore a second threshold is observed at the $\tilde{A}$ state adiabatic energy. No increase in SiF_3^+ production is observable at the SiF_4^+ $\tilde{C}\,^2T_2$ state energy of 642 Å (19.3 eV). This is disappointing because this state has an unmeasurably low fluorescence quantum yield[16] [Section 4.A(i)], so non-radiative decay must dominate.

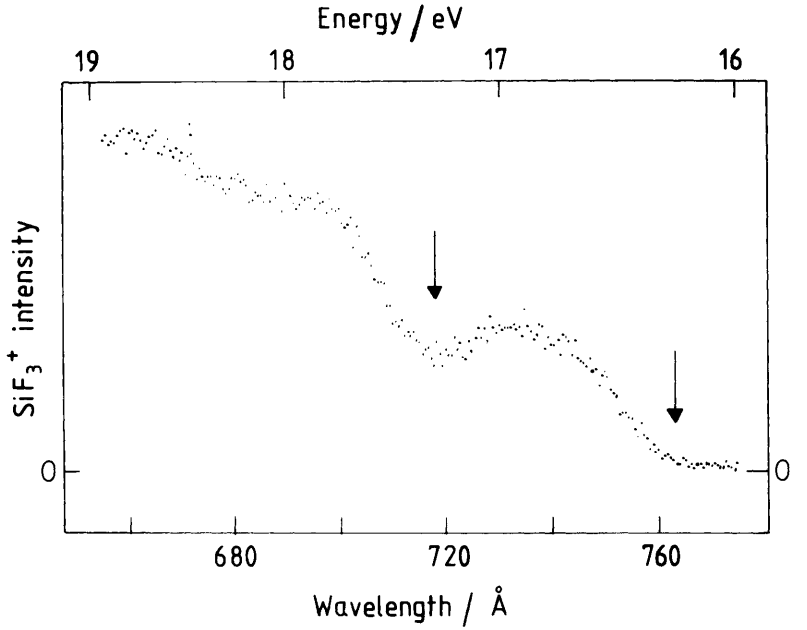

Figure 15 *Photoionization yield curve of* SiF_3^+ *from* SiF_4 *in the range* 655—775 Å. *The two thresholds for* SiF_3^+ *production are marked*
(Reproduced by permission from *J. Chem. Phys.*, 1990, **93**, 3299)

Energetically $SiF_3^+ + F$ is the only accessible channel (Table 1), and therefore an increase in SiF_3^+ signal would be expected at this energy. This highlights particularly well one limitation of having no electron energy analysis in our PEPICO apparatus. At any photon energy where several electronic states of SiF_4^+ are accessible, the SiF_3^+ signal has contributions from all those states which fragment to $SiF_3^+ + F$. Since the sum of the partial ionization cross-sections into SiF_4^+ $\tilde{X}$, $\tilde{A}$, and $\tilde{B}$ is much greater than into $\tilde{C}$ around 20 eV,[42] we are attempting to observe a very small increase in SiF_3^+ signal against a very much larger signal already present. No new thresholds are observed at the energy of SiF_4^+ $\tilde{D}$ (576 Å or 21.5 eV) because this state decays radiatively with unity fluorescence quantum yield.

B. Fragmentation of the Chlorides of Group IV.[10]—The results for fragmentation of CCl_4 when excited by vacuum UV photons are perhaps the most interesting of the group IV tetrahalide ions studied. Figure 16 (see opposite p. 461) shows that three ions are present over the photon range studied (560—790 Å), CCl^+ for

[42] B. W. Yates, K. H. Tan, G. M. Bancroft, L. L. Coatsworth, and J. S. Tse, *J. Chem. Phys.*, 1985, **83**, 4906.

$\lambda < 645$ Å (19.2 eV), CCl_2^+ for $\lambda < 760$ Å (16.3 eV), and CCl_3^+ over the complete wavelength range, and it should be noted that the adiabatic energies of CCl_4^+ $\tilde{D}$ and $\tilde{C}$ are 19.3 and 16.3 eV respectively (Table 1). Thus CCl_2^+ turns on at the $\tilde{C}$ state adiabatic energy, CCl^+ at the $\tilde{D}$ state, and these non-radiative fragmentation rates are presumably fast enough to dominate any much slower radiative decay. Thus the fluorescence quantum yields of these two states are unmeasurably low [Section 4.A(ii)]. The question immediately arises as to whether these decay channels are unique, *e.g.* does CCl_4^+ $\tilde{D}$ only fragment to CCl^+? This is difficult to answer with total confidence because any competing fragmentation pathway of either state to, say, $CCl_3^+ + Cl$ would be difficult to observe in the CCl_3^+ ion yield curve because of the lack of energy analysis in the electron TOF spectrometer. However, if the channels are unique, and assuming all three ions are collected with equal efficiency, then at any photon energy above the CCl_4^+ $\tilde{D}$ state the ratio of the CCl^+ to CCl_2^+ to CCl_3^+ intensities should equal the ratio of σ_D to σ_C to $(\sigma_X + \sigma_A + \sigma_B)$, where σ_i is the partial ionization cross-section into electronic state i. The ratio of the ion yields is easily obtained by computer integration of the three peaks in the TOF spectra. Unfortunately cross-section data are very limited in this photon range,[43] and as a general statement this work has highlighted the need for much more experimental data on partial ionization cross-sections of valence states of polyatomic ions in the vacuum UV. The comparison cannot therefore be made. However, we comment that this is one advantage of using a TOF mass spectrometer rather than a quadrupole as a means of ion detection in a photofragment experiment, since in the former case quantitative comparisons can be made accurately between the intensities of the different fragment ions.

The results for $SiCl_4^+$ and $GeCl_4^+$ fragmentation are not so informative. Photofragmentation was studied from below the energy of the $\tilde{C}$ state to above that of the $\tilde{D}$ state, and in both cases only two ions are clearly present, the parent ion MCl_4^+ and the trichloride ion MCl_3^+. The $\tilde{C}$ state of both parent ions fluoresce with a long radiative lifetime (Section 4.B), so no new fragmentation channels are to be expected at the $\tilde{C}$ state adiabatic energies; this is indeed the case. Unlike the fluorides, the $\tilde{D}$ states of MCl_4^+ do not fluoresce, so a non-radiative fragmentation pathway is to be expected. No new channel is immediately apparent from the colour maps. However by careful comparison of the TOF spectra above and below the $\tilde{D}$ state adiabatic energies (Section 2), a threshold to $SiCl_2^+$ is observed for energies above $SiCl_4^+$ $\tilde{D}$, and two thresholds to $GeCl^+$ and $GeCl_2^+$ for energies above $GeCl_4^+$ $\tilde{D}$. The channels are weak presumably because the partial ionization cross-sections of both $SiCl_4$ and $GeCl_4$ into their $\tilde{D}$ ionic states are very low.

C. Fragmentation of the Bromides of Group IV.[38]—Fragmentation of both $SiBr_4$ and $GeBr_4$ has been studied from below the energy of the $\tilde{X}$ ionic state to above that of the $\tilde{D}$ state. Both gratings of the Seya were needed to cover this large

[43] T. A. Carlson, M. O. Krause, F. A. Grimm, P. Keller, and J. W. Taylor, *J. Chem. Phys.*, 1982, 77, 5340.

range (*ca* 500—1200 Å) The data were recorded only very recently at Daresbury, and they have not yet been properly analysed, however the broad features are apparent from the colour maps Not surprisingly $SiBr_4^+$ and $GeBr_4^+$ appear to show similar fragmentation pathways Like the chlorides two main peaks are observed, MBr_4^+ and MBr_3^+ The parent ion peak turns on at the $\tilde{X}$ ionic state adiabatic energy, whereas the tribromide ion turns on at the $\tilde{A}$ state energy The monobromide ion MBr^+ turns on at the $\tilde{D}$ adiabatic energy with the dibromide ion appearing at even higher energy As expected, no new channel is observed at the energy of the $\tilde{C}$ state, since both $SiBr_4^+$ and $GeBr_4^+$ $\tilde{C}$ decay radiatively

The MBr_3^+ results are the most interesting since they suggest that the $\tilde{A}$ states of MBr_4^+ are repulsive, dissociating promptly by loss of one bromine atom to $MBr_3^+ + Br$ In other words the thermodynamic dissociation energy for $MBr_3^+ + Br$ lies close to or more probably below the MBr_4^+ $\tilde{A}$ adiabatic energy, but above the $\tilde{X}$ state energy This is exactly the situation with CCl_4^+, $SiCl_4^+$, and $GeCl_4^+$ [10] (Table 1) The energetics of the dissociation channels of $SiBr_4^+$ and $GeBr_4^+$ were given in one of our earlier papers,[23] and the surprising point to emerge then was that the best available thermodynamics placed the $SiBr_3^+ + Br$ channel *ca* 5 eV higher than that to be expected We commented at the time that this was a difficult observation to believe, and that an energy scanning PEPICO experiment was needed to determine the true dissociation energy of $SiBr_4$ into $SiBr_3^+ + Br$ The preliminary analysis of this experiment does indeed confirm that the $SiBr_3^+ + Br$ channel lies between 10 9 and 11 5 eV, and not at 16 2 eV as suggested earlier [23] Full details will appear later [38] There is no obvious discrepancy between the preliminary analysis of $GeBr_4^+$ photodissociation and the thermodynamics in reference 23

D. Fragmentation of SF_6^+.[39]—We have made an extensive study of photofragmentation of SF_6 excited with VUV photons from 440—810 Å The wavelength range extends from below the energy of the ground state of SF_6^+ to above that of the highest valence electronic state SF_6 and CF_4 belong to closely related molecular point groups (T_d is a sub-group of O_h), their molecular orbitals and photoelectron spectra have many similarities, and both have repulsive ionic ground states dissociating promptly by loss of a fluorine atom to SF_5^+ and CF_3^+ respectively [44] Therefore as with CF_4^+, we hoped to observe radiative decay from high lying valence states of SF_6^+ As mentioned in Section 4 A(v) no photon emission could be detected in our fluorescence excitation apparatus, therefore all valence states of SF_6^+ must decay non-radiatively by fragmentation

Berkowitz[45] has used conventional PIMS to study photofragmentation of SF_6, but was limited to photon wavelengths > 600 Å due to the nature of the ionization source (the helium continuum) Thus the products from dissociation of the higher energy valence states of SF_6^+ were uncertain Our detailed results can

[44] I G Simm C J Danby J H D Eland and P I Mansell *J Chem Soc Faraday Trans* 1976 **72** 426

[45] Ref 12 p 325

be found elsewhere,[39] and only a brief summary is given here. Thresholds for SF_5^+ production are observed at the adiabatic energies of the $\tilde{X}\,^2T_{1g}$ and first two excited states $\tilde{A}/\tilde{B}\,^2T_{1u}/^2T_{2u}$ of SF_6^+. These states lie 1.5 and 2.7 eV above the $SF_5^+ + F$ thermodynamic dissociation channel. The ion yield curve for SF_4^+ turns on at the adiabatic energy of the third excited state of SF_6^+, $\tilde{C}\,^2E_g$; this lies 1.2 eV above the lowest channel forming SF_4^+. SF_3^+ thresholds are observed at the adiabatic energies of both the fourth ($\tilde{D}\,^2T_{2g}$) and fifth ($\tilde{E}\,^2T_{1u}$) excited states of SF_6^+, whilst SF_2^+ turns on at the adiabatic energy of the highest valence ionic state of SF_6^+ ($\tilde{F}\,^2A_{1g}$). Thus in all cases SF_n^+ ($n = 2$—5) shows a threshold at an adiabatic energy of an electronic state of SF_6^+, and not at the lowest thermodynamic dissociation channel forming that ion. This is exactly what we observe with CF_4^+, and arises because of the totally repulsive nature of the ground electronic state. Dissociation *via* high vibrational levels of this state is therefore not a route for fragment ion production.

As with CCl_4^+ (Section 5.B) the question arises whether these fragmentation channels are unique; for example, does SF_6^+ $\tilde{C}$ only fragment to SF_4^+ or is there a competing channel to SF_5^+? Partial ionization cross-sections or photoelectron branching ratios are available for all the valence states of SF_6^+,[46] so a comparison can now be made between the relative yields of SF_5^+, SF_4^+, SF_3^+ with that expected from the cross-section data. The latter results overestimate the yields of SF_3^+ and SF_4^+ to SF_5^+, and this may be evidence that the $\tilde{C}$, $\tilde{D}$, and $\tilde{E}$ states of SF_6^+ do fragment to SF_5^+ in competition with dissociation to SF_4^+ and SF_3^+. From the widths of the peaks in the TOF spectra, KE releases have been measured in SF_5^+, SF_4^+, and SF_3^+. Interpretation of the values for SF_5^+ and SF_4^+ are consistent with dissociation of SF_6^+ $\tilde{X} + \tilde{A}/\tilde{B}$ and $\tilde{C}$ to ($SF_5^+ + F$) and ($SF_4^+ + F_2$) respectively. The SF_3^+ value cannot be used to extract a unique total KE release because dissociation of SF_6^+ to SF_3^+ is necessarily many bodied, involving more than two products.

6 Conclusions

I have not attempted to give a full review of the applications of tunable vacuum UV photons from a synchrotron source to gas phase molecular photophysics. Instead I have concentrated on its application to study a particular area of chemical physics into which I came from a spectroscopic background. Much work has been done on fragmentation of both singly- and double-charged ions using a synchrotron as a photon source, and the full range of coincidence techniques has been applied to a large number of diatomics and polyatomics. However, rather to our surprise, no other group has combined the powerful combination of the PEPICO coincidence technique with the step-by-step tunability of the photon source as described in this review. Fluorescence excitation spectroscopy using synchrotrons has generally been limited to wavelengths above the lithium

[46] B. M. Addison-Jones, K. H. Tan, B. W. Yates, J. N. Cutler, G. M. Bancroft, and J. S. Tse, *J. Electron Spectrosc. Relat. Phenom.*, 1989, **48**, 155.
[47] L. C. Lee, J. C. Han, C. Ye, and M. Suto, *J. Chem. Phys.*, 1990, **92**, 133.

fluoride cut-off ($\lambda > 106$ nm), precluding the need for differential pumping, and only one other group (L C Lee and co-workers, refs 32, 47) is working in the vacuum UV down to 50 nm

I believe that the main conclusions to come out of this work and future areas of investigation are as follows

(1) The observation of radiative decay from high lying valence electronic states of polyatomic ions is not confined to the highly symmetrical tetrahedral species like CF_4^+ Fluorescence has now been observed from excited states of BF_3^+ and BCl_3^+ (of D_{3h} symmetry)[35] and CF_3H^+ and CF_3Cl^+ (of C_{3v} symmetry),[27] and we are confident that this effect will be observed in other species

(2) Referring specifically to the group IV tetrahalides MX_4^+, it would be interesting to understand why for a given X the carbon species behaves differently from silicon and germanium, and for given M the fluoride behaves differently from the chloride and bromide The different decay properties of the $\tilde{D}\,^2A_1$ state of the chloride/bromide ion from that of the fluoride could be a consequence of spin–orbit coupling effects in the heavier species creating non-radiative decay channels *via* doublet–quartet coupling These problems can only be addressed if detailed positions of the potential curves of both doublet and quartet valence states of MX_4^+ are known *Ab initio* calculations have recently been reported on the energies of the five valence doublet electronic states of MF_4^+,[48] but there have been no calculations yet on the quartet states or on any of the states in MCl_4^+ and MBr_4^+

(3) All the molecular ions studied have repulsive or scarcely bound ground and low-lying excited electronic states These states arise from electron removal from halogen non-bonding $p\pi$ orbitals (where the halogen p orbitals are orthogonal to the M—halogen bonds), and tend to have structureless photoelectron bands By contrast the states from which radiative decay has been observed are formed by electron removal from M—halogen σ-bonding orbitals, and often have vibrationally resolved structured photoelectron bands This is surprising, because it is not at all obvious why the latter ionic states tend to have deep minima in their potential curves and hence are more likely to decay radiatively by the relatively slow process of photon emission than the former states

(4) It is difficult to estimate accurately fluorescence quantum yields of radiating electronic states by the method described in Section 4 A(i), and data for partial ionization cross-sections need to be known $\Phi_{h\nu}$ is best estimated by a coincidence technique, *e g* the PIFCO method,[5] and we are building an apparatus to perform these measurements Perhaps the strongest indication of a fluorescence quantum yield of unity is the absence of variation of τ with excitation energy (Section 4 B), but it can only be an indication

(5) The combination of a continuously tunable photon source and TOF detection for fragment ions is a powerful tool for investigating non-radiative fragmentation of electronic states of polyatomic ions We believe our technique has several advantages over conventional PIMS[12] (which were described in

[48] R A Bearda H R R Wiersinga J F M Aarts and J J C Mulder *Chem Phys* 1989 **137** 157

Section 2), which help to countenance the difficulties of working within limited time schedules at a synchrotron source. Fragment thresholds are observed to ± 5 Å in most of our work. This resolution is determined by the slit width of the Seya monochromator, and in principle thresholds could be measured much more accurately if unlimited beam time was available.

(6) The most interesting point to come out of the fragmentation work is that when the ionic ground state is repulsive (*e.g.* in CF_4^+ and SF_6^+ [44]) fragment ions have appearance thresholds at the adiabatic energies of electronic states of the parent ion, and not at the lowest thermodynamic threshold forming that ion. This is not the expected pattern for large polyatomic ions, but rather that which is observed with diatomic ions. For polyatomics the conventional view is that the initial ionization event (whether by electrons or photons) serves only to create the molecular ion in a range of electronic states, but equilibration takes place so rapidly that one need only consider the density of vibrational states of the electronic ground state of the ion in determining the fragmentation pattern. This pattern can be determined by statistical methods [e.g. quasi-equilibrium theory (QET)] where one calculates the probability for dissociation of a bond to form a fragment ion at a certain total energy. In QET the fragment ions have thresholds at their thermodynamic energy, and any excess energy appears mainly as internal energy of the fragments, not as translational energy. However with CF_4^+ and SF_6^+, in effect because the ionization potentials of CF_3 and SF_5 are small compared to CF_4 and SF_6, the $\tilde{X}$ state of these ions lies above the lowest dissociation channel to CF_3^+ or $SF_5^+ + F$. These states are therefore repulsive. QET cannot apply to the fragmentation of CF_4^+ or SF_6^+, and one can only form the smaller fragment ions (*e.g.* CF_2^+, SF_4^+) by non-radiative decay of excited states of CF_4^+ or SF_6^+ which lie *above* their thermochemical energies. The excess energy is (partially) converted into KE release in the fragments, and in the ions this manifests as a broadening in the width of the TOF peak. As mentioned several times in this review, accurate determination of these KE releases is not possible in our apparatus because the internal state of the parent ion initially populated by the vacuum UV photon is not defined uniquely. This is most easily accomplished with a threshold electron detector, and this modification is being incorporated into the new apparatus we are currently building.

Acknowledgements. It is a pleasure to acknowledge the help of my research group (J. C. Creasey, Dr. P. A. Hatherly, I. R. Lambert, and Dr. S. M. Mason) in this work. I am especially grateful to Professor K. Codling and Dr. L. Frasinski of Reading University for a fruitful collaboration, since the fragmentation work uses a modified form of one of their apparatus, and to Dr. M. Stankiewicz of Krakow University who wrote much of the software for this experiment. I would like to thank Dr. A. Hopkirk of the Daresbury Laboratory who was involved in the design and construction of the fluorescence excitation apparatus, and others at Daresbury (especially Drs. M. Hayes, D. M. P. Holland, D. A. Shaw, and J. B. West) for help and encouragement. The financial support of the Science and Engineering Research Council is acknowledged.

Note added in proof. Fluorescence following vacuum UV photoexcitation of BF_3 has very recently been reported by Lee *et al.* (*Phys. Rev. A*, 1990, **42**, 424). They see the same 'BF_2' bands that we observe (Figure 10) at low photon energies, but do not observe emission from excited states of the parent ion BF_3^+ (unlike our results of Figure 11). They measure lifetimes for the two BF_2 bands which are microsecond range. These are indirect measurements, and are much greater than our values (Table 3) of 16 and 47 ns. The reasons for these discrepancies are as yet unclear.